ROYAL INSTITUTE
OF TECHNOLOGY

Determination of a Gravimetric Geoid Model of Sudan Using the KTH Method

Ahmed Abdalla

Master's of Science Thesis in Geodesy No. 3109
TRITA-GIT EX 09-01

Division of Geodesy

Royal Institute of Technology (KTH)

100 44 Stockholm, Sweden

January 2009

TRITA-GIT EX 09-01

ISSN 1653-5227

ISRN KTH/GIT/EX--09/001-SE

Dedicated to my parents for their valuable sacrifices to provide me, brothers and sisters a quality of life with full motivation in higher education.

… I love you more than words could ever say …

Abstract

The main objective of this study is to compute a new gravimetric geoid model of Sudan using the KTH method based on modification of Stokes' formula for geoid determination. The modified Stokes' formula combines regional terrestrial gravity with long-wavelength gravity information provided by the global gravitational model (GGM). The collected datasets for this study contained the terrestrial gravity measurements, digital elevation model (DEM), GPS/levelling data and four global gravitational Models (GGMs), (*EGM96, EIGEN-GRACE02S, EIGEN-GL04C and GGM03S*).

The gravity data underwent cross validation technique for outliers detection, three gridding algorithms (*Kriging, Inverse Distance Weighting and Nearest Neighbor*) have been tested, thereafter the best interpolation approach has been chosen for gridding the refined gravity data. The GGMs contributions were evaluated with GPS/levelling data to choose the best one to be used in the combined formula.

In this study three stochastic modification methods of Stokes' formula (*Optimum, Unbiased and Biased*) were performed, hence an approximate geoid height was computed. Thereafter, some additive corrections *(Topographic, Downward Continuation, Atmospheric and Ellipsoidal)* were added to the approximated geoid height to get corrected geoid height.

The new gravimetric geoid model (KTH-SDG08) has been determined over the whole country of Sudan at 5′ x 5′ grid for area ($4^\circ \le \phi \le 23^\circ$, $22^\circ \le \lambda \le 38^\circ$). The optimum method provides the best agreement with GPS/levelling estimated to 29 *cm* while the agreement for the relative geoid heights to 0.493 *ppm*. A comparison has also been made between the new geoid model and a previous model, determined in 1991 and shows better accuracy.

Keywords: *geoid model, KTH method, stochastic modification methods, modified Stokes' formula, additive corrections.*

Acknowledgements

Firstly, I wish to express my deepest gratitude to my supervisor Dr. Huaan Fan for introducing and motivating me to physical geodesy field and for his valuable advices, genuine support and guidance which helped me a lot to finish this study. I would also like to thank my examiner Professor Lars Sjöberg, I am very fortunate to be one of your students.

Special thanks are due to Professor Derek Fairhead and Matthew Stewart, Geophysical Exploration Technology (GETECH), University of Leeds, UK for providing Sudan gravity data. Also my thanks are due to Eng. Mubarak Elmotasim and Eng. Suliman Khalifa for providing the GPS/levelling data, I would also like to thank Dr. Artu Ellmann for introducing software of solving least-squares parameters. I am also thankful to my classmate Ilias Daras for sharing knowledge and fruitful discussions with valuable comments regarding this study.

My heartfelt gratitude to staff members of division of geodesy at KTH for the friendly environment and permanent readiness to help at any time during the entire Master's Programme , in particular, PhD student Mehdi Eshagh for answering various questions relevant this study. A special thank to Ms. Sofia Norlander, Students office at School of Architecture and the Built Environment at KTH. Thanks for the friendly people, the Swedish people. I would like to thank my corridor mates, particularly, Annika for the time she dedicated to revise and correct my English writing, I would also like to thank Anna, Celesté, Marcus and Siddig Elmukashfi for the nice times and the good memories.

I would like to thank Professor Abdalla Elsadig and Eng. Salah Abukashawa, Sudan National Survey Authority for their warm welcoming during my visit to Sudan. I am also indebted to my BSc supervisor Dr. Mohamed Osman Adam, University of Khartoum-Department of Surveying Engineering, for encouragement and motivation during my undergraduate studies. I would like to thank Dr. Hassan Fashir, although we have not yet met, but hopefully we will meet in the future. Many thanks are due to Professor Tag Elsir Bashir and Geologist Walid Siddig.

My sincere thanks are due to my classmates in IMPGG and to Sudanese students at KTH, particularly, I am grateful to my classmate Elbashir Elhassan for a nice companionship since the first day we met at KTH. I am also indebted to my friends in Sudan (no one mentioned, no one forgotten) for the sweet times during my last visit.

Last but not least, I owe immense gratitude to my Father (the pillar of my strength and the source of my inspiration) for his unlimited support and encouragement, his patience and optimism undoubtedly have overcome many tough times during my study. I am so indebted to my mother where my life came from. I am also indebted to my brothers, sisters, uncles, aunts, nephews and nieces for their kind regards and thoughtfulness my study circumstances, with a special thank to my elder brother Khalid for partial support. Thanks for being a wonderful family! It is great that a day has come to make some dreams a reality.

Stockholm, October 2008

Ahmed Abdalla

Table of Contents

List of Figures

List of Tables

List of Abbreviations and Acronyms

BGI	Bureau Gravimétrique International
CHAMP	CHAllenging Minisatellite Payload
DEM	Digital Elevation Model
DWC	Downward Continuation
DOT	Dynamic Ocean Topography
EGM96	Earth Gravitational Model (degree/order 360/360)
EIGEN-GL04C	GRACE Gravity Model (degree/order 360/360)
EIGEN-GRACE02S	GRACE Gravity Model (degree/order 150/150)
ERS-1	European Remote Sensing Satellite
GEM-T1	Goddard Earth Model
GEOSAT	GEOdetic SATellite
GETECH	Geophysical Exploration Technology
GFZ	Deutsches GeoForschungsZentrum
GGM	Global Gravitional Model
GGM03S	GRACE Gravity Model (degree/order 180/180)
GNSS	Global Navigation Satellite System
GIS	Global Information System
GMSE	Global Mean Square Error
GOCE	Gravity field and Steady State Ocean Circulation Exporter
GPS	Global Positioning System
GRACE	Gravity Recovery and Climate Experiment
GRAS	Geological Research Authority of Sudan
GRS80	Geodetic Reference System 1980

KTH	Kungliga Tekniska högskolan
KTH-SDG08	KTH- Sudanese Geoid 2008
IMPGG	International Master Programme in Geodesy and Geoinformatics
LSM	Least Squares Modification
LSMS	LSM of Stokes' Formula
MSL	Mean Sea Level
MSE	Mean Square Error
NASA	National Aeronautics and Space Administration (USA)
NIMA	National Imagery and Mapping Agency (USA)
NRL	Naval Research Laboratory (USA)
NWC	National Water Corporation (Sudan)
SGG	Satellite Gravity Gradiometry
SLR	Satellite Laser Ranging
SRTM	Shuttle Radar Topography Mission
SST	Satellite-to-Satellite Tracking
SVD	Singular Value Decomposition
TDRSS	Tracking and Data Relay Satellite System
TOPEX	TOPography EXperiment for Ocean Circulation
T-SVD	Truncated Singular Value Decomposition
T-TLS	Truncated Total Least Squares
USGS	US Geological Survey

Chapter 1

Introduction

1.1 Background

Geodesy from the Greek literally stands for Earth (geo-) dividing (-desy). Modern geodesy concerns with the determination of the size and the shape of the Earth and its gravity field. Geodesy also concerns determination of the precise positions of points or objects on and near the earth surface with defined geodetic reference system on national or global datums. Practically, geodesy could be divided into three subfields: geodetic positioning, gravity field study and geodynamics.

One of the most fundamental concepts in geodesy is the geoid, which is defined as an equipotential surface that coincides with the mean sea level (MSL) and extends below continents. In some places (e.g. the Netherlands and the Black Sea) it is actually above the Earth surface. The geoid surface is much smoother than the natural Earth surface despite of its global undulations (changes). It is very close to an ellipsoid of revolution, but more irregular. Hence it is well approximated by the ellipsoid. Historically, the geoid has served as reference surface for geodetic levelling. The geoid height or geoidal undulation *(N)* describes by the separation of the geoid from the ellipsoid of revolution. Due to the irregularity of the geoid, it cannot be described by a simple mathematical function.

High-resolution geoid models are valuable to geodesy, surveying, geophysics and several geosciences, because they represent the datums to height differences and gravity potential. Moreover, they are important for connection between local datums and the global datum, for purposes of positioning, levelling, inertial navigation system and geodynamics.

The impact of wide and rapid use of the Global Navigation Satellite System (GNSS) has revolutionized the fields of surveying, mapping, navigation, and Geographic Information Systems (GIS) and replaced the traditional time-consuming approaches. In particular, GPS offers a capability of making geodetic measurements with a significant accuracy that

previously required ideal circumstances, weather and other special preparations. Further, the new accuracy is achieved efficiently and economically than was possible before GPS. The GPS is three-dimensional; this implies that it supplies heights as well as horizontal positions. The given height in this system is computed relative to the ellipsoid; hence, it is called *ellipsoidal height*. However, height from spirit levelling is related to the gravity field of the Earth, it is called *orthometric height*. The geoid height is the difference between the ellipsoidal and the *orthometric height*. It is well known that the *orthometric height* can be obtained without levelling by using the *ellipsoidal* and *geoidal height*. The obtained *orthometric height* must be determined with high accuracy. Therefore, the determination of a high-resolution geoid has become a matter of great importance to cope possibly with accuracy level of height from GPS. Hence, it is possible to say that gravimetric geoid models offer the third dimension to GPS.

Not all regions of the world contain gravity field measurements based on terrestrial and airborne methods. Meanwhile, the gravitational field of the Earth can be determined globally and with high precision and resolution by means of dedicated satellite gravity missions:

- Satellite-to-Satellite Tracking (SST) in high-low mode being realized by the "Challenging Minisatellite Payload" (CHAMP) mission.
- Satellite-to-Satellite Tracking in low-low mode being realized by the "Gravity Recovery and Climate Experiments" (GRACE), and
- A combined Satellite Gravity Gradiometry (SGG) the objective of the "Gravity field and Steady State Ocean Circulation Exporter" (GOCE) mission.

The satellite missions are expected to provide significant improvements to the global gravity field by one to three orders and also contribute to resolving the medium wavelength part (around 100 km) of the gravity field of the Earth, so as to achieve high resolution geoid.

1.2 Objectives of the thesis work

The main objective of this study is to determine a gravimetric geoid model of Sudan using the method of The Royal Institute of Technology (KTH) developed by Professor L.E Sjöberg (2003d). This method is based on least-squares modification of Stokes' formula (LSMS). Herein the modified Stokes' function is applied instead of the original one, which has a very

significant truncation bias unless a very large area of integration is used around the computation point (Sjöberg and Ågren 2002). In KTH method, the surface gravity anomaly and GGM are used with Stokes' formula, providing an approximate geoid height. Previously, several corrections must be added to gravity to be consistent with Stokes' formula. In contrast, here all such corrections (Topographic, Downward Continuation, Ellipsoidal and Atmospheric effects) are added directly to the approximate geoid height. This yields the corrected geoid height, which will be tested against geometrical geoid height derived from the GPS/levelling data, so as to assess the precession of the gravimetric geoid model.

1.3 Thesis Structure

This thesis consists of six Chapters, including this first introductory Chapter; the other Chapters are summarized as below:

- **Chapter two**

  Glances the least-squares modification of Stokes' formula and shows the core concept.
- **Chapter three**

  Shows how the additive corrections computed in order to be added directly to the approximate geoid height in KTH method.
- **Chapter four**

  Details the data acquisition and identifies all datasets required by the combined method of geoid computation.
- **Chapter five**

  Presents a new gravimetric geoid model (KTH-SDG08) over the target area as well as the additive corrections, it also shows some numerical results with the geoid accuracy in absolute and relative senses.
- **Chapter six**

  Summarizes conclusions with discussions and concluding remarks.

Chapter 2

Least-squares modification of Stokes' formula

2.1 Modification of Stokes' formula

In 1849 a well-known formula was published by George Gabriel Stokes. It is therefore called *Stokes' formula* or *Stokes' integral*. It is by far the most important formula in physical geodesy because it is used to determine the geoid from gravity data. The geoid determination problem is expressed as a boundary value problem in the potential theory based on Stokes' theory. Hence, the *gravitational disturbing potential T* can be computed as:

$$T = \frac{R}{4\pi} \iint_{\sigma} S(\psi) \Delta g \, d\sigma, \tag{2.1}$$

where R is the mean Earth radius, ψ is the geocentric angle, Δg is gravity anomaly, $d\sigma$ is an infinitesimal surface element of the unit sphere σ and $S(\psi)$ is the Stokes function. $S(\psi)$ can be expressed as a series of Legendre polynomial $P_n(\cos\psi)$ over the sphere:

$$S(\psi) = \sum_{n=2}^{\infty} \frac{2n+1}{n-1} P_n(\cos\psi) \tag{2.2}$$

$S(\psi)$ can also take the closed expression:

$$S(\psi) = \frac{1}{\sin\left(\frac{\psi}{2}\right)} - 6\sin\frac{\psi}{2} + 1 - 5\cos\psi - 3\cos\psi \ln\left(\sin\frac{\psi}{2} + \sin^2\frac{\psi}{2}\right) \tag{2. 3}$$

The *disturbing potential (T)* is the difference between the actual gravity potential on the geoid surface W and the normal potential value U on the reference ellipsoid surface. Another famous formula in physical geodesy, Bruns' formula (cf. Bruns 1878) which relates the geoidal undulation N to the disturbing potential T:

2.1 Modification of Stokes' formula

$$N = \frac{T}{\gamma} \tag{2.4}$$

where γ stands for the normal gravity on the reference ellipsoid

By substitution we get Stokes' formula:

$$N = \frac{R}{4\pi\gamma} \iint_{\sigma} S(\psi)\Delta g d\sigma \tag{2.5}$$

The surface integral in Stokes' formula (2.5) has to be applied over the whole Earth. However, practically the area is limited to a small spherical cap $\sigma_\circ$ around the computation point due to limited coverage of available gravity anomaly data. Hence, the surface integral cannot be extended all over the Earth. Accordingly the surface integral has to be truncated to gravity anomaly area $\sigma_\circ$ and then we get an estimator of the geoid height:

$$N = \frac{R}{4\pi\lambda} \iint_{\sigma_\circ} S(\psi)\Delta g d\sigma \tag{2.6}$$

The difference between geoid height in Equation (2.5) and the new estimator in Equation (2.6) δN is called the truncation error of Stokes' formula:

$$\delta N = -\frac{R}{4\pi\gamma} \iint_{\sigma-\sigma_\circ} S(\psi)\Delta g d\sigma \tag{2.7}$$

where $(\sigma - \sigma_\circ)$ is called the remote zone (the area outside the gravity area). Molodensky *et al* (1962) proposed that the truncation error of the remote zone can be reduced when Stokes' formula combines the terrestrial gravity anomalies and long-wavelength (up to degree *M*) as a contribution of the Global Gravitational Model (GGM).

With satellites era, it becomes possible to generate geoid models in global sense. When combining information from the GGM with Stokes' integration over local gravity data, regional geoid models may be estimated (e.g. Rapp and Rumell 1975). In Geoid modeling two components should be considered: long-wavelength component provided by GGM (using spherical harmonics) and short-wavelength component from local gravity

observations. By using local gravity data, Stokes' formula will be truncated to inner zone. This causes truncation errors due to the lack of the gravity data in remote zones; these errors could be ignored or reduced by modifying Stokes' Kernel.

The approaches of kernel modifications are broadly classified into two categories, *stochastic* and *deterministic. Stochastic methods* are used to reduce the global mean square error of truncation errors as well as random errors of the GGM and gravity data. Stochastic methods presented by Sjöberg (1980, 1981, 1984, 1991, 2001) beside the attempt by Wenzel (1981, 1983). On the other hand, *deterministic methods* aim to minimize the truncation errors caused by poor coverage of the terrestrial gravity observations. *Deterministic methods* presented by Wong and Gore (1969), Demitte (1967), Vaníček and Kleusberg (1987), Heck and Gründg (1987) and Featherstone *et al* (1998). Accuracy of the geoid estimators depends on the extent of the local gravity anomalies around the computation point, therefore the choices of the cap σ of spherical radius $(\psi_\circ)$ are region dependent. It is difficult to choose most suitable kernel modification approach or cap of spherical radius without comparing the gravimetric geoid heights with GPS/levelling geoid, which is the essential step of gravimetric geoid computation process.

Sjöberg (1984a, b, 1986, 1991) used least-squares principle to decrease the expected global mean error of modified Stokes' formula. Sjöberg (2004) utilized the error of the GGM and terrestrial gravity data to derive the modification parameters of Stokes' kernel in a local least-squares sense. By taking the advantage of the orthogonality of spherical harmonics over the sphere, Equation (2.6) can be defined by two sets of modification parameters, S_n and b_n:

$$\tilde{N} = \frac{c}{2\pi}\iint_{\sigma_o} S^L(\psi)\Delta g d\sigma + c\sum_{n=2}^{M} b_n \Delta g_n^{EGM}, \qquad (2.8)$$

where $b_n = \left(Q_n^L + s_n^*\right)\dfrac{c_n}{c_n + dc_n}$ *for* $2 \le n \le M$, $c = R/2\gamma$ and Δg_n^{EGM} is the Laplace harmonics of degree n and calculated from an EGM (Heiskanen and Moritz 1967 p.89).

$$\Delta g_n^{EGM} = \frac{GM}{a^2}\left(\frac{a}{r}\right)^{n+2}(n-1)\sum_{m=-n}^{n} C_{nm}Y_{nm}, \qquad (2.9)$$

where a is the equatorial radius of the reference ellipsoid, r is the geocentric radius of the computation point, GM is the adopted geocentric gravitational constant, the coefficients C_{nm} are the fully normalized spherical harmonic coefficients of the disturbing potential provided by the GGM, and Y_{nm} are the fully normalized spherical harmonics (Heiskanen and Moritz 1967, p.31).

The modified Stokes's function is expressed as

$$S^L(\psi) = \sum_{n=2}^{\infty} \frac{2n+1}{n-1} P_n(\cos\psi) - \sum_{n=2}^{L} \frac{2n+1}{2} s_n P_n(\cos\psi), \tag{2.10}$$

where the first term on the right-hand side is the original Stokes function, $S(\psi)$ in terms of Legendre polynomials.

Generally the upper bound of the harmonics to be modified in Stokes's function, L is arbitrary and not necessarily equal to the GGMs' upper limit M . The truncation coefficients are:

$$Q_n^L = Q_n - \sum_{k=2}^{L} \frac{2k+1}{2} s_k e_{nk}, \tag{2.11}$$

where Q_n denotes the Molodensky's truncation coefficients:

$$Q_n = \int_{\psi_\circ}^{\pi} S(\psi) P_n\left(\cos\psi\right) \sin(\psi) d\psi, \tag{2.12}$$

and e_{nk} are functions of $\psi_o : e_{nk}\left(\psi_0\right) = \int_{\psi^0}^{\pi} P_n(\cos\psi) P_k(\cos\psi) \sin\psi d\psi$.

By utilizing the error estimates of the data, and some approximations (both theoretical and computational), we arrive at an estimate of the geoid height that we call the approximate geoidal height, which can be written in the following spectral form (cf. Sjöberg 2003d, Equation 8a):

$$\tilde{N} = c\sum_{n=2}^{\infty}\left(\frac{2}{n-1} - Q_n^L - s_n^*\right)\left(\Delta g_n + \varepsilon_n^T\right) + c\sum_{n=2}^{M}\left(Q_n^L + s_n^*\right)\left(\Delta g_n + \varepsilon_n^S\right), \tag{2.13}$$

where ε_n^T and ε_n^S are the spectral errors of the terrestrial and GGM derived gravity anomalies, respectively. The modification parameters are:

$$s_n^* = \begin{cases} s_n & if\ \ 2 \le n \le L \\ 0 & n > L \end{cases} \tag{2.14}$$

Based on the spectral form of the "true" geoidal undulation N (Heiskanen and Moritz 1967, p. 97):

$$N = c\sum_{n=2}^{\infty}\frac{2\Delta g_n}{n-1}, \tag{2.15}$$

The expected global MSE of the geoid estimator $\tilde{N}$ can be written as:

$$\begin{aligned} m_{\tilde{N}}^2 &= E\left\{\frac{1}{4\pi}\iint_{\sigma}\left(\tilde{N} - N\right)^2 d\sigma\right\} \\ &= c^2\sum_{n=2}^{M}\left(b_n^2 dc_n\right) + c^2\sum_{n=2}^{\infty}\left[b_n^* - Q_n^L(\psi_0) - s_n^*\right]^2 c_n + c^2\sum_{n=2}^{\infty}\left[\frac{2}{n-1} - Q_n^L(\psi_0) - s_n^*\right]^2\sigma_n^2, \end{aligned} \tag{2.16}$$

where $E\{\}$ is the statistical expectation operator, c_n are the gravity anomaly degree variances, σ_n^2 are the terrestrial gravity anomaly error degree variances, dc_n are the GGM derived gravity anomaly error degree variances and:

$$b_n^* = \begin{cases} b_n & if\ \ 2 \le n \le L \\ 0 & otherwise \end{cases}, \tag{2.17}$$

The first, middle and last term of the right hand side of Equation (2.16) are due to effects of GGM errors, truncation errors and erroneous terrestrial data, respectively. According to the previous assumption of the errors of the all data. The norm of the total error can be obtained by adding their partial contribution. However, in practice the GGM and ground gravity data are often correlated especially when the GGM is a combined (satellite data, terrestrial and

altimetry data). This correlation can be avoided when using satellite only harmonics (not combined GGM) in low degrees of the model.

To obtain the least-squares Modification (LSM) parameters, Equation (2.16) is differentiated with respect to s_n, i.e. $\partial m_{\tilde{N}}^2 / \partial s_n$. The resulting expression is then equated to zero, and the modification parameters s_n are thus solved in the least-squares sense from the linear system of equations (Sjöberg 2003d):

$$\sum_{r=2}^{L} a_{kr} s_r = h_k, \quad k = 2,3,.....,L, \tag{2.18}$$

where

$$a_{kr} = \sum_{n=2}^{\infty} E_{nk} E_{nr} C_n + \delta_{kr} C_r - E_{kr} C_k - E_{kr} C_r, \tag{2.19}$$

and

$$h_k = \Omega_k - Q_k C_k + \sum_{n=2}^{\infty} \left(Q_n C_n - \Omega_k \right) E_{nk}, \tag{2.20}$$

where

$$\Omega_k = \frac{2\sigma_k^2}{k-1}, \tag{2.21}$$

$$\delta_{kr} = \begin{cases} 1 & if\ k = r \\ 0 & otherwise \end{cases} \tag{2.22}$$

$$C_k = \sigma_k^2 + \begin{cases} c_k dc_k / \left(c_k + dc_k \right) & if\ \ 2 \le k \le M \\ c_k & if\ \ k > M \end{cases}, \tag{2.23}$$

$$E_{nk} = \frac{2k+1}{2} e_{nk}\left(\psi_0 \right), \tag{2.24}$$

The modification parameters s_n vary, depending on the quality of local gravity data, the chosen radius of integration (ψ^0) and the characteristics of the GGM. The system of equations in Equation (2.18) is *ill-conditioned* in optimum and unbiased LSM solutions and well-conditioned in bias solution. The *ill-conditioned* system of equations cannot be solved by standard methods like Gaussian elimination. To overcome this problem, Ellmann (2005a) and Ågren (2004a) used the standard Singular Value Decomposition *(SVD)* procedure provided e.g. by Press et al. (1992). After the numerical solution of s_n, the corresponding coefficients b_n are computed.

2.2 Signal and noise degree variances

The main purpose of this section is accordingly to show how realistic signal degree variances are possibly computed and chosen. Signal degree variances are to be used for the construction of GGMs and are also utilized in the determination of modification coefficients b_n.

2.2.1 Gravity anomaly degree variances (c_n)

The degree variance c_n can be computed by using spherical harmonic coefficients C_{nm} and S_{nm} of the disturbing potential, gravitational constant GM and equatorial radius of the GGM a as follows:

$$c_n = \frac{(GM)^2}{a^4}(n-1)^2 \sum_{m=0}^{n}\left(C_{nm}^2 + S_{nm}^2\right) \tag{2.25}$$

In practice, the infinite summation in Equation (2.16) must be truncated at some upper limit of the expansion, in this study n_{max}=2000. The higher degree c_n could be generated synthetically to meet the spectral characteristics of the Earths' gravity field. In order to determine degree variances for the gravity field, Ågren (2004) has investigated three different degree variances models [e.g. Kaula 1963, Tscherning and Rapp 1974 and Jekeli and Motritz 1978]. With regard to how they can model the high degree information, the Tscherning and Rapp model (1974) for estimation of the signal gravity anomaly degree

variances yields the most realistic values and gives reasonable RMS values for what is obtained in regional geoidal height (Ågren 2004a). It is admitted by Tscherning (1985) that the horizontal gradient variance $G_\circ$ is too high for areas with topography below 500 *m* and it is too low in areas with high mountains and ocean trenches.

The model is nevertheless useful in a global mean squares sense. Moreover, Moritz pointed out that the gradient is highly sensitive to smoothing operations (see Moritz 1980, sect. 23). Since Tscherning and Rapp (1974) model was a strong candidate used in Ågren (2004), herein we also use it in our study. Tscherning and Rapp (1974) is defined by:

$$c_n = \alpha \frac{(n-1)}{(n-2)(n+24)} \left(\frac{R_B^2}{R^2} \right)^{n+2}, (n \geq 3) \tag{2.26}$$

where the coefficients $\alpha = 425.28\ mGal^2$ and $R = 6371$ km, and the radius of Bjerhammer sphere $R_B = R$-1.225 km. However, this model is valid just for the gravity field uncorrected for any topographic effects.

2.2.2 Geopotential harmonic error degree variances (dc_n)

The error degree variances can be estimated from using standard error of the potential coefficients $d_{C_{nm}}$ and $d_{S_{nm}}$ (e.g. Rapp and Pavlis, 1990):

$$dc_n = \frac{(GM)^2}{a^4}(n-1)^2 \sum_{m=0}^{n} \left(d_{C_{nm}}^2 + d_{S_{nm}}^2 \right) \tag{2.27}$$

The coefficients $d_{C_{nm}}$ and $d_{S_{nm}}$ are a natural part of many GGMs. Combined GGMs such as EGM96 (Lemoine at al., 1998) utilize rather heterogeneous datasets. Naturally, the accuracy of these models depends on geographic coverage of gravity data contribution in the solution. However, the variance by Equation (2.20) is global and not necessarily representative for the target area. The resulting dc_n looks too pessimistic, so for more realistic estimates over such regions the variance dc_n could be re-scaled by applying some empirical factors.

2.2.3 Terrestrial data error degree variances (σ_n^2)

The degree variances σ_n^2 are used for estimating the global Mean Square Error (MSE); it can be estimated by the *reciprocal distance model*. According to Moritz H (1980) σ_n^2 can be estimated from degree covariance function $C(\psi)$ can be estimated from the simple relation according to Sjöberg (1986, Chapter 7):

$$\sigma_n^2 = c_T(1-\mu)\mu^n, \quad 0 < \mu < 1, \tag{2.28}$$

where the constants c_T and μ can be estimated from the knowledge of an isotropic covariance function. The covariance function $C(\psi)$ can be presented in closed form (Moritz H., 1980, p.174), using the ordinary expression for reciprocal distance which leads to:

$$C(\psi) = c_T\left\{\frac{1-\mu}{\sqrt{1-2\mu\cos\psi+\mu^2}} - (1-\mu) - (1-\mu)\mu\cos\psi\right\}. \tag{2.29}$$

Equation (2.22) is just a rough model for computing σ_n^2 and it is utilized for determining the constant μ. For $\psi = 0$ the variance by Equation (2.21) becomes:

$$C(0) = c_T\mu^2, \tag{2.30}$$

and thus it follows that:

$$C(\psi_\circ) = \frac{1}{2}c_T\mu^2. \tag{2.31}$$

The parameters c_T and c_μ can be computed for given value of the variance σ_n^2 and knowledge of and knowledge of the covariance function $C(\psi)$. Some numerical technique is needed to compute μ from $\psi = 0$. The solution with $\mu = 0.99899012912$ (associated with $\psi_\circ = 0.1^\circ$) is used in a software designed by Ellmann (2004). The constant μ is found from trivial iterations, inserting μ into Equation (2.23) c_T is completely determined and σ_n^2 is then calculated. In Ellmann's software the user is asked to insert the value of $C(0)$ as

the accuracy of the gravity anomalies in the grid. After investigating different $C(0)$ values, $C(0)$ has been chosen to be 9 $mGals^2$.

2.3 Theoretical accuracy of the geoid height

The internal accuracy of the geoid heights is taken as a global mean square error of the geoid estimators. It is important to note that changing the initial values, e.g. $\psi_\circ$ or $C(0)$ could enhance or deteriorate the *global mean square error* (GMSE) which is derived for the optimum method of the least-squares as follows:

$$m_{\hat{N}}^2 = f - c^2 \sum_{k=2}^{L} \hat{s}_k h_k, \tag{2.32}$$

where $\hat{s}_k$ are the least-squares solutions to s_k and f is given by:

$$f = c^2 \left[\sum_{n=2}^{n_{\max}} \left(\frac{2}{n-1} - Q_n^L \right)^2 \sigma_n^2 + \sum_{n=2}^{M} Q_n^2 \frac{c_n dc_n}{c_n + dc_n} + \sum_{n=2}^{n_{\max}} Q_n^2 c_n \right]. \tag{2.33}$$

For this study, the following values are taken for geoid computation $n_{max} = 2000$, maximum degree of modification and expansion $L = M = 120$ (for *GGM*) and truncation radius $\psi_\circ = 3^o$ the global root mean square error is estimated to about 6 cm which is too optimistic and does not match exactly with actual results. The expected MSE is only a theoretical estimator, which needs to be confirmed by some external datasets and practical computations. The external assessment of different modification methods can be achieved by comparing the geoid model with GPS/levelling data, see Section 5.4.

Chapter 3

Additive Corrections to the Geoid Model

The Stokes' formula presupposes that the disturbing potential is harmonic outside the geoid. This simply implies that there are no masses outside the geoid surface, and that must be moved inside the geoid or completely removed in order to apply Stokes' formula. This assumption of the forbidden masses outside the geoid (bounding surface) is necessary when treating any problem of physical geodesy as a *boundary-value problem* in potential theory.

Additionally, the application of Stokes' formula needs gravity to be observed or reduced at the sea level which represents the bounding surface or the integral boundary. The gravity reduction to the sea level surface implies a change of gravity corresponding to topographic and atmospheric direct effect on the geoid. After applying Stokes' formula in determination the gravimetric geoid, the effect of restoring the topography and atmospheric masses (the indirect effect) is accounted. Stokes' formula applies to spherical reference surface. Therefore the entering is given on the sphere. In the approximation of the geoid given by a global reference ellipsoid, there is a deviation of about 100 m, which causes a systematic error of about several decimeters in geoid height when neglecting the flattening of the ellipsoid. The correction of the gravity anomaly for the direct effect must be analytically downward continued (reduced) to the sea level, this step is called *downward continuation* (DWC).

In the KTH computational scheme for geoid determination (Sjöberg 2003c) on the surface, gravity anomalies and GGM are used to determine the approximate geoid height $\tilde{N}$, then all corrections are added to $\tilde{N}$ separately. In contrast to conventional methods by means of gravity reductions, the forbidden masses are treated before using Stokes' formula which is the purpose of the various gravity reductions.

The computational procedure of the KTH scheme for determination of the geoid height $\tilde{N}$ is given by the following formula:

$$\hat{N} = \tilde{N} + \delta N_{comb}^{Topo} + \delta N_{DWC} + \delta N_{comb}^{a} + \delta N_{e} \quad (3.1)$$

where δN_{comb}^{Topo} is the combined topographic correction, which includes the sum of direct and indirect topographical effects on the geoid, δN_{DWC} is the downward continuation effect, δN_{comb}^{a} is the combined atmospheric correction, which includes the sum of the direct and indirect atmospherical effects and δN_{e} is the ellipsoidal correction for the spherical approximation of the geoid in Stokes' formula to ellipsoidal reference surface.

3.1 The Combined Topographic Correction

The combined topographic effect is the sum of direct and indirect topographical effect on the geoid; it can be added directly to the approximate geoidal height value derived from equation as follows:

$$\delta N_{comb}^{Topo} = \delta N_{dir} + \delta N_{indir} \approx -\frac{2\pi G\rho}{\gamma} H^2, \quad (3.2)$$

where $\rho = 2.67\ g/cm^3$ is the mean topographic mass density and H is the orthometric height. This method is independent of selected type of topographic reduction (Sjöberg 2000 and 2001a). By summation of direct and indirect effects the reduction effect mostly diminishes. Furthermore, the direct topographic effect which usually affected by a significant terrain effect is cancelled in the combined effect on the geoid.

The combined topographic correction is dependent on the density of topographic masses. As Sjöberg emphasized in 1994, if the density of topographic masses varies within 5%, the propagated geoid error could be as large as a few decimeters, globally. For instance, areas below 1300 m, the combined topographic correction is within 1 *cm*, therefore for some areas the knowledge of topographical densities is not a problem. In this study a constant mass density value $2.67\ g/cm^3$ is considered due to a difficulty of obtaining reliable density information, as normally a constant density is used in many traditional approaches. If lateral density variation of topographic masses is adequately known, then more accurate results can be obtained by Sjöberg (2000, Equation 113) and Ellmann and Sjöberg (2002, Equations 10 and 11).

The Equation (3.2) is very simple and computer efficient as it is valid with slopes of topography less than 45º. Because of the fact that rough surface gravity anomalies are integrated in KTH approach, some important comments must be considered in using the method. Errors of Stokes' integration (discretisation error) when sampling the mean surface Δg anomalies from gravity point data-due to loss of shortwave-length information. These errors can be reduced significantly by using special interpolation technique, for more details see (Ågren 2004 and Kiamehr 2005). In addition a good *Digital Elevation Model* (DEM) should be available with at least the same resolution as the interpolated grid or denser.

3.2 The Downward Continuation Correction

The analytical continuation of the surface gravity anomaly to the geoid is a necessary correction in application of Stokes' formula for geoid estimation. The necessity of this is when the topographic effect is reduced; the observed surface gravity anomalies must be downward continued to the geoid.

DWC has been done in different methods, but the most common method is the inversion of Poison's integral, which reduces the surface gravity anomaly for direct topographic effect and then continue the reduced gravity anomaly downward to the sea level. This method has been studied by Martinec and Vaníček (1994a), Martinec (1998), Hunegnaw (2001). A new method for DWC is introduced by Sjöberg (2003a). This method avoids the downward continued gravity anomaly and considers directly the DWC effect on the geoidal height. Accordingly, the DWC effect on the geoidal height can be written as follows:

$$\delta N_{dwc} = \frac{c}{2\pi} \iint_{\sigma_0} S_L(\psi)\left(\Delta g^* - \Delta g\right) d\sigma, \tag{3.3}$$

where Δg is the gravity anomaly at the surface computation point P and Δg^* is the corresponding quantity downward continued to the geoid. The final formulas for Sjöberg's DWC method for any point of interest P based on LSM parameters can be given by (for more details, see Ågren 2004):

$$\delta N_{dwc}(P) = \delta N_{DWC}^{(1)}(P) + \delta N_{DWC}^{L1,Far}(P) + \delta N_{DWC}^{L2}(P), \tag{3.4}$$

where

$$\delta N_{dwc}^{(1)}(P) = \frac{\Delta g(P)}{\gamma} H_P + 3\frac{\zeta_P^0}{r_P} H_P - \frac{1}{2\gamma}\frac{\partial \Delta g}{\partial r}\bigg|_P H_P^2, \tag{3.5}$$

The notation ζ_P^0 is used to denote an approximate value of height anomaly. Due to diminutive value of $\delta N_{dwc}(P) = 1\,mm$ that corresponds to an error of 1 m for $H_P = 2$ km and $r_P = 6375$ km, it is comfortable to adopt:

$$\zeta_P^0 \approx \frac{c}{2\pi}\iint_{\sigma_o} S^L(\psi)\Delta g d\sigma + c\sum_{n=2}^{M}\left(s_n + Q_n^L\right)\Delta g_n^{EGM}, \tag{3.6}$$

$$\delta N_{dwc}^{L(1),Far}(P) = c\sum_{n=2}^{M}\left(s_n^* + Q_n^L\right)\left[\left(\frac{R}{r_P}\right)^{n+2} - 1\right]\Delta g_n(P), \tag{3.7}$$

and

$$\delta N_{dwc}^{L(2)}(P) = \frac{c}{2\pi}\iint_{\sigma_0} S_L(\psi)\left(\frac{\partial \Delta g}{\partial r}\bigg|_P \left(H_P - H_Q\right)\right) d\sigma_Q, \tag{3.8}$$

where $r_P = R + H_P$, σ_0 is a spherical cap with radius $\psi_\circ$ centered around P and it should be the same as in modified Stokes' formula, H_P is the orthometric height of point P and gravity gradient $\frac{\partial \Delta g}{\partial r}\Big|_P$ in point P can be computed based on Heiskanen and Moritz (1967,p.115):

$$\frac{\partial \Delta g}{\partial r}\bigg|_P = \frac{R^2}{2\pi}\iint_{\sigma_0}\frac{\Delta g_Q - \Delta g_P}{l_0^3} d\sigma_Q - \frac{2}{R}\Delta g(P), \tag{3.9}$$

where $l_o = 2R\sin\frac{\psi_{PQ}}{2}$.

In Equation (3.7) $\Delta g_n(P) = \frac{n-1}{R}\sum_{m=-n}^{n} A_{nm} Y_{nm}(P)$. Here A_{nm} is the potential coefficient related to the fully normalized spherical harmonic (cf. Heiskanen and Moritz 1967, p. 31). Equation (3.8) can be adequately treated in the same way of the evaluation of the modified Stokes' integration.

3.3 The Ellipsoidal Correction

Geoid determination by Stokes' formula holds only on spherical boundary, the mean Earth sphere with radius R. Since the geoid is assumed to be the boundary surface for the gravity anomaly, the ellipsoid is a better approximation for it. A relative error of 0.3% in geoid determination caused by the deviation between the ellipsoid and the geoid, reaching thus several centimeters. This deviation is a consequence of geoid irregularities. Hence for accurate geoid model it is important to estimate ellipsoidal correction. Ellipsoidal correction has been studied by different authors through the years, e.g. Molodensky *et al* (1962), Moritz (1980), Martinec and Grafarend (1977), Fei and Siders (2000) and Heck and Seitz (2003). A new Integral solution was published by Sjöberg (2003b). The ellipsoidal correction for the original and modified Stokes' formula is derived by Sjöberg (2003c) and Ellmann and Sjöberg (2004) in a series of spherical harmonics to the order of e^2, where e is the first eccentricity of the reference ellipsoid. The approximate ellipsoidal correction can be determined by a simple formula, (for more details, see Sjöberg 2004):

$$\delta N_e \approx \psi_o \left[\left(0.12 - 0.38 \cos^2 \theta \right) \Delta g + 0.17 \tilde{N} \sin^2 \theta \right]. \qquad (3.10)$$

where ψ_o is the cap size (in units of degree of arc), θ is geocentric co-latitude, Δg is given in mGal and $\tilde{N}$ in m. It is concluded by Ellmann and Sjöberg (2004) that the absolute range of the ellipsoidal correction in LSM of Stokes' formula does not exceed the cm level with a cap size within a few degrees.

3.4 The Atmospheric Correction

Due to the fact that the atmospheric masses outside the geoid surface cannot be removed completely, hence we must consider correction for the forbidden atmospheric masses and added as additional term to fulfill boundary condition in Stokes' formula. In the *International Association of Geodesy* (IAG) approach, the Earth is supposed as a sphere with spherical atmospheric ring, while the topography of the Earth is completely neglected Moritz (1992). Accordingly some direct and indirect effects to gravity anomaly must be accounted; the indirect effect is too small that is usually neglected. Sjöberg (1998, 1999b, 2001a and 2006) emphasized that the application of IAG approach using a limited cap size especially in

3.4. The Atmospheric Correction

Stokes' formula can cause a very significant error in zero order term (more than 3m). In the KTH scheme, the combined atmospheric effect δN^a_{comb} can be approximated to order H by (Sjöberg and Nahavandchi 2000):

$$\delta N^a_{comb}(P) = -\frac{2\pi R\rho_\circ}{\gamma}\sum_{n=2}^{M}\left(\frac{2}{n-1} - s_n - Q^L_n\right)H_n(P) - \frac{2\pi R\rho_\circ}{\gamma}\sum_{n=M+1}^{\infty}\left(\frac{2}{n-1} - \frac{n+2}{2n+1}Q^L_n\right)H_n(P), \qquad (3.11)$$

where $\rho_\circ$ is the density at sea level ρ°, $\left(\rho^\circ = 1.23\times10^{-3}\, g/cm^3\right)$ multiplied by the gravitational constant G, $\left(G = 6.673\times10^{-11}\, m^3/kg^1s^2\right)$, γ is the mean normal gravity on the reference ellipsoid and H_n is the Laplace harmonic of degree n for the topographic height:

$$H_n(P) = \sum_{m=-n}^{n} H_{nm}\overline{Y}_{nm}(P), \qquad (3.12)$$

The elevation H of the arbitrary power ν can be presented to any surface point with latitude and longitude (ϕ,λ) as:

$$H^\nu(\phi,\lambda) = \sum_{m=0}^{\infty}\sum_{m=-n}^{n} H^\nu_{nm}Y_{nm}(\phi,\lambda), \qquad (3.13)$$

where H^ν_{nm} is the normalized spherical harmonic coefficient of degree n and order m, it can be determined by the spherical harmonic analysis:

$$H^\nu_{nm} = \frac{1}{4\pi}\iint_\sigma H^\nu(\phi,\lambda)Y_{nm}(\phi,\lambda)\,d\sigma, \qquad (3.14)$$

The normalized spherical harmonic coefficients $\left(H^\nu_{nm}\right)$ used in this study, were given by Fan (1998) and they were computed to degree and order 360.

Chapter 4

Data Acquisition

4.1 Terrestrial gravity surveys in Sudan

Gravity surveys in Sudan started in 1975 and were very important in discovery of the Mesozoic rift basins of Sudan. Before that time, few gravity measurements had been made in Sudan (except the Red Sea), and a very little seismic data had been collected to support the geodetic techniques conducted for groundwater exploration (Texas Instruments Inc.,1962), (*Hunting Geology and Geophysics limited*, 1970), (Strojexport, 1971,72, 75, 76,1977). In addition *Techno export* (1971-78) conducted gravity studies in Red Sea hills for mineral exploration and *Farwa* (1978) conducted a gravity surveying in EL-Gezira.

From 1975 to 1984 *Chevron Oil Company* has covered Muglad, Melut and Southern Blue Nile rift with gravity surveys. In 1979 the University of Leeds with cooperation of *Geological and Mineral Resources Department* of Sudan carried out gravity survey in central Sudan and western Sudan to fill two large gabs in the existing coverage not covered by *Chevron* (Brown. et al, 1984); (Birmingham, 1984). In 1981, *Total Oil Company* conducted gravity in southern Sudan in part of Muglad rift. From 1982 to 1987, Sun took over Philips areas of northern Sudan and conducted a gravity survey which covered most of central Sudan. For hydro geological purposes in 1984 , *Bonifca Geo export* conducted a gravimetric survey in northern Sudan with cooperation of the Sudanese National Water Corporation (NWC) to cover area of about 41,500 km^2 (Bonifca, 1986). In petroleum promotion project, *Robert Research International* (RRI) with collaboration of *Geological Research Authority of Sudan* (GRAS) carried out a major regional gravity survey of north east Sudan which is a remote desert region. On the Red Sea marine *AGIP Oil* conducted a gravity survey designed to assess the hydrological potential of this region. Meanwhile, the only offshore data are ship-borne gravity collected by the *Compagnei Geophysique General* under contract with the Saudi-Sudanese Red Sea commission in 1976 (Izzeldinm 1987) for the exploration of the metallifero- us muds for more information see (Ibrahim A, 1993).

4.1.1 Gravity data validation and gridding

The terrestrial gravity data for this study was provided by *Geophysical Exploration Technology* (GETECH) group, University of Leeds. The provided database comprises 23509; the area 22 E to 39 E and 4 N to 24 N includes 5′ x 5′ bouguer and free air anomaly and height grids, Gravity station locations and technical details of surveys. Additional data from *Bureau Gravimétrique International* (BGI) comprises 2645 gravity observations covering some parts of the neighboring countries; hence the total number of both datasets becomes 26154. Simply we can say the available data represents about 33% of area of computation.

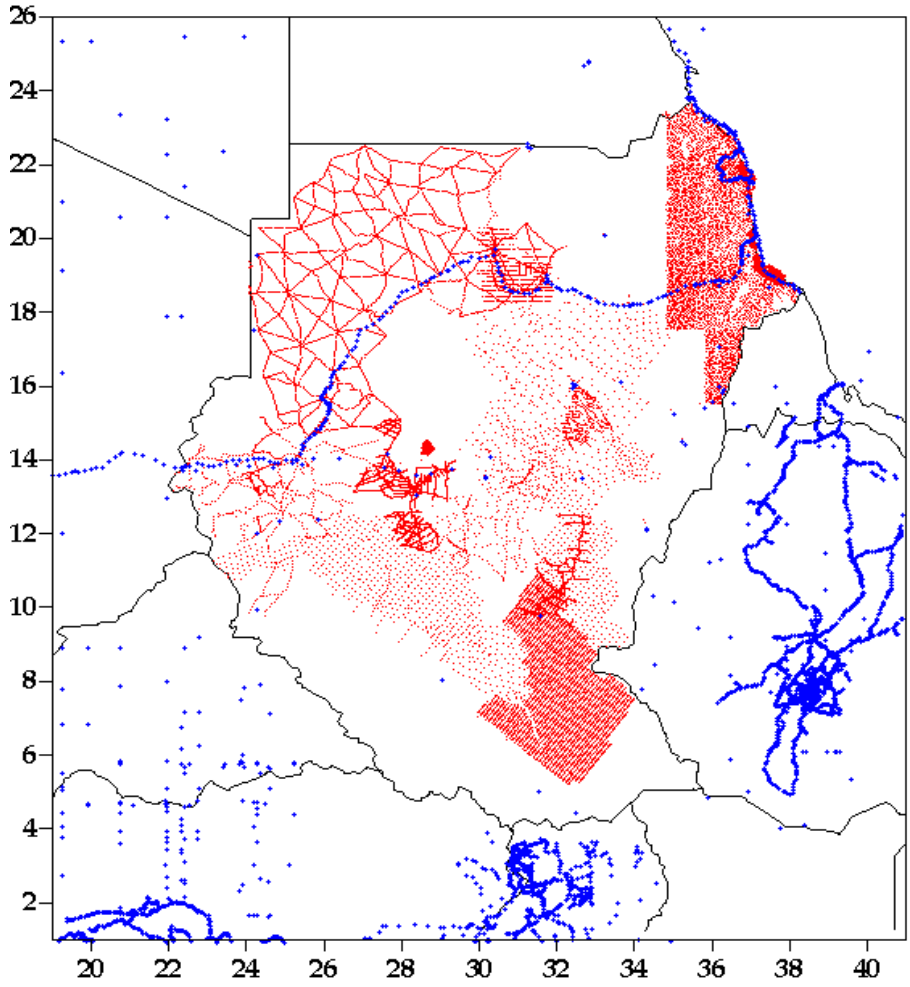

Figure 4.1: Distribution of the gravity anomaly data (GETECH and BGI data showed in red and blue colours, respectively).

This makes abundantly clear that there is data shortage in terrestrial observations, which causes a significant limitation on the geoid model accuracy, nevertheless the accuracy of the

computational method of geoid determination. From the information of data acquisition in Section 4.1, obviously, it has been collected by different organizations with different intentions, thus, strongly makes the data quality is arguable. In other words, it may include erroneous points. Apparently, data needs to be validated carefully before used in geoid computation. Both GETECH and BGI data were used as one dataset for cleaning of gravity anomaly to avoid data corruption in geoid result. Two tests based on *cross validation* approach have been implemented for the available data to detect and eliminate gross errors.

The cross-validation method is introduced by S.Geisser and W.F. Eddy (1979). It is an established technique for estimating the accuracy of the data. To calculate the predicted value of Δg, cross-validation removes a point required for prediction (*test point*) and calculates the value of this location using the mean values of the surrounding points (*training points*). The predicted and observed values at the location of the removed point are compared. This process is repeated for a second point, and so the rest. The observed and predicted values are compared for all points and then the difference between predicted and observed values is the interpolation error $\delta\Delta g$.

$$\delta\Delta g = \Delta g_{pre} - \Delta g_{obs}, \tag{4.1}$$

where Δg_{pre} is the predicted value of the gravity anomaly, Δg_{obs} is the observed gravity anomaly.

Because of random scatter of the gravity datasets, an interpolation is needed to be applied, for obtaining a regular data grid. Three gridding techniques e.g. *kriging* using the Linear variogram model (slope=1, anisotropy: ratio=1, angle=0), *inverse distance weighting* (Power=2, smoothing factor=0, anisotropy: ratio=1) and *nearest neighbor* were investigated, in order to find which is the best one that gives the minimum standard deviation for the cross-validation approach and hence to be used in the final gridding.

Kriging gives a minimum residuals standard deviation (27 mGal) than *inverse distance weighting* (41 mGal) and *nearest neighbor* (32 mGal), therefore Kriging is selected in our study to dense our grid. *Kriging* is a geostatistical method, that comprises a set of linear regression routines reduce the estimation variance from a predefined covariance model. It assumes that

4.1.1. Gravity data validation and gridding

the interpolated parameter can be treated as a regionalized variable which is intermediate between a truly random variable and a completely deterministic variable according to its variance from one location to the next. Surfer software from Golden Software Inc, Colorado was used to generate the results of the investigation in this part of this study.

Bouguer gravity anomalies were used for outliers' detection because they are smoother and less topography-dependent than free-air gravity anomalies. Wherever rough topographic masses are found, the free-air anomalies will be also rough due to sensitivity, therefore the interpolation never accomplished properly. The tolerance to detect outliers can be simply fixed by drawing the histogram of the absolute values of the interpolation error of the all points. A keen alteration of the slope then represents the tolerance point; points underneath this value are accepted. In this study outliers were detected at 60 mGal, this means that points with prediction error greater than 60 mGal are considered as outliers and then deleted. From the test result it is found that 213 points had prediction error greater than 60 mGal and deleted from the dataset.

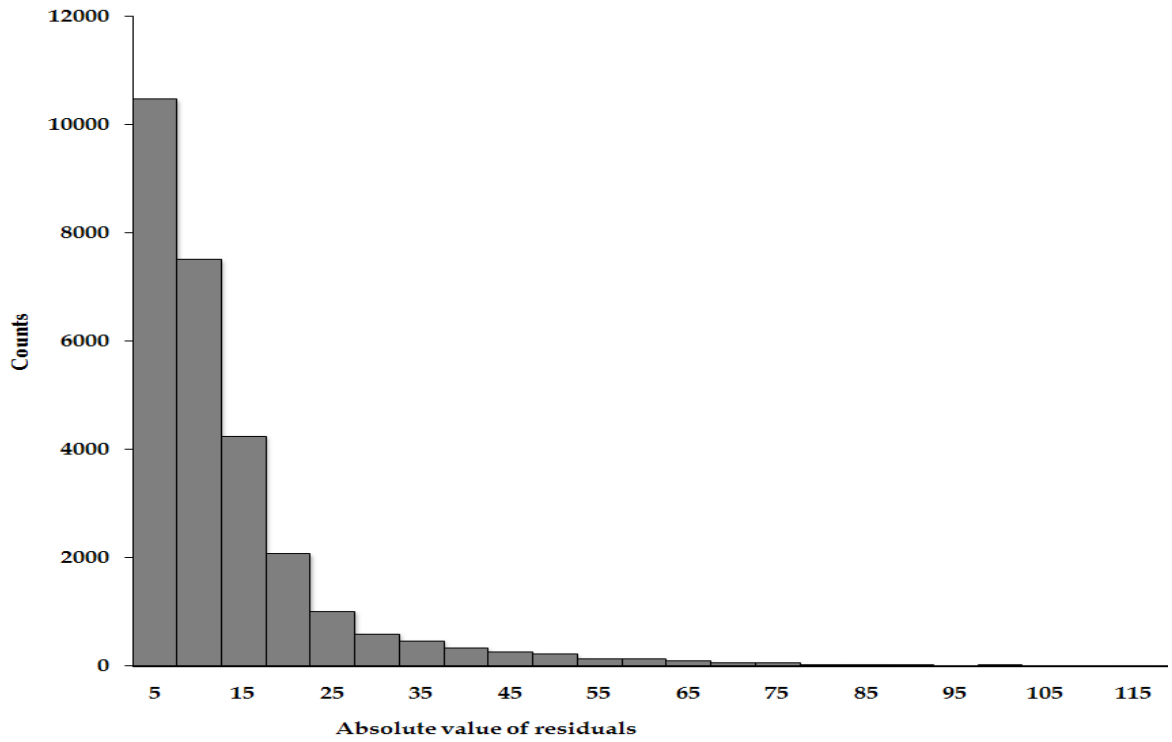

Figure 4.2: Histogram of the absolute values of residuals of bouguer anomalies interpolation.

4.1.2 Molodensky gravity anomalies

Conventionally, in geoid determination by means of gravity reductions, the geoid serves as a basis for establishing the position of points of the Earth surface. This means that all geodetic measurements are reduced to the geoid. The big constraint of this approach is that it requires the density of masses at any point between the geoid and the Earth surface to be known, which is obviously unattainable. For this reason Molodensky introduced a new theory to overcome this problem in Stokes' theory. He used Earth surface and the telluroid to describe the anomalous gravity field, similarly to geoid and reference ellipsoid in Stokes theory. Gravity anomaly of Molodensky can be defined as the difference between the actual gravity on the Earth surface and the normal gravity on the telluroid.

$$\Delta g_A = g_A - \gamma_B, \tag{4.2}$$

where point *A* lies on the surface of the Earth and point *B* along the ellipsoidal normal, at the telluroid. Numerically Δg_A is close to the free air gravity anomaly on the geoid. If point A has normal height H_A, then the normal gravity γ_B on the telluroid can be calculated from the normal gravity γ_Q on the ellipsoid:

$$\gamma_B = \gamma_Q - 2\gamma_e\left(\frac{H_A}{a}\right)\left[1 + f + m + \left(-3f + \frac{5}{2}m\right)\sin^2\phi\right] + 3\gamma_e\left(\frac{H_A}{a}\right)^2, \tag{4.3}$$

where *a* is the equatorial radius, γ_e is the normal gravity at the equator, γ_Q is computed by *Somigliana's* formula as follows

$$\gamma_Q = \gamma_e \frac{1 + k\sin^2\phi}{\sqrt{1 - e^2\sin^2\phi}} \text{ where, } k = \frac{b\gamma_p}{a\gamma_e} - 1 \text{ and } e = \sqrt{\frac{a^2 - b^2}{a^2}},$$

$m = \left(\omega^2 a^2 b\right)/GM = 0.003449786000308$ (Constant for GRS80) and ϕ the geodetic latitude of the point, f the geometric flattening of the reference ellipsoid.

A second test for the detection of outlier points was done by comparing gravity anomalies of Molodensky with free-air gravity anomalies computed by EIGEN-GL04C combined gravitational model. The absolute value of the differences is shown in Figure 4.3.

4.1.2. Molodensky gravity anomalies

It is found from the second test that 20 points were considered as oultiers and therefore they were deleted. The differences were expected to be large due to the fact that terrestrial gravity data contains all frequencies of the gravity field, whereas the GGMs do not. Additionally, the terrestrial gravity data are highly susceptible to medium- and long-wavelength errors due to errors in vertical geodetic datums, which are used to compute gravity anomalies, and to gravimeter drift, which tends to accumulate over long distances (cf. Featherstone et al., 2002).

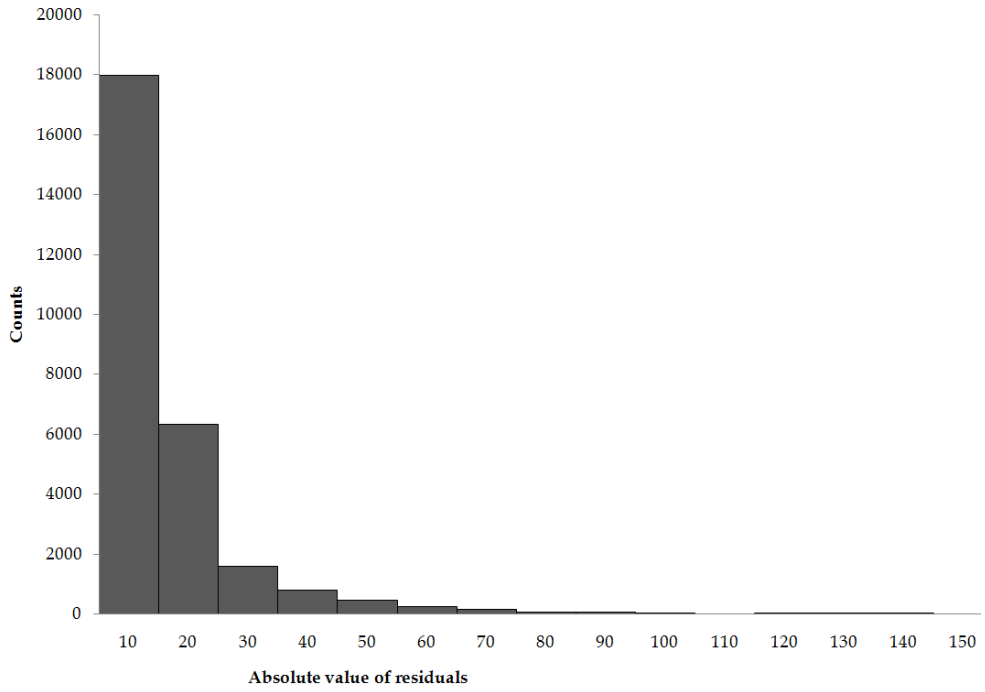

Figure 4.3: Histogram of the absolute values of residuals of difference between Molodensky gravity anomalies and EIGEN-GL04C free-air gravity anomaly.

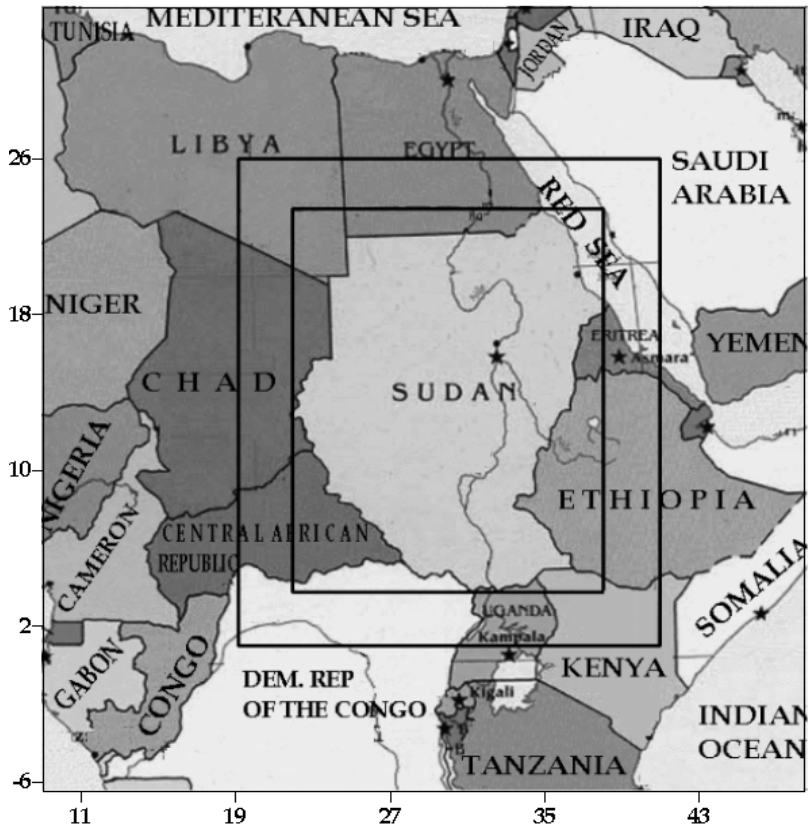

Figure 4.4: Sudan area fenced by the smaller rectangle, outer rectangle fences Sudan area at spherical distance of 3°.

Finally, a gridded data with 5′ x 5′ resolution is distributed over the study area ($4^\circ \le \phi \le 23^\circ,\ 22^\circ \le \lambda \le 38^\circ$) and also extended to the outside in offset of 3°, the outer rectangle in Figure 4.4 to be well adapted to the moving integration cap radius at any truncated point of computation with spherical distance $\psi_\circ = 3^\circ$. The deleted points are 233, while the remaining are 25921. The gridded area had blocks without gravity data due to the shortage of gravity coverage. Compatible free air anomalies were computed from EIGEN-GL04C to fill the empty blocks. A total number of the grid blocks is 79488, blocks with gravity data are 24837 while 54651 were filled by gravity anomalies computed from EIGEN-GL04C gravitational model.

4.2 The Digital Elevation Model (DEM)

A DEM that used in present study is a gridded topography with a block size of 30" x 30" from the *Shuttle Radar Topography Mission* (SRTM) is released by the *National Aeronautics and Space Administration* (NASA) in 2003. The DEM extends to cover the target area with the proposed 3° adapted offset as $(19^\circ \le \lambda \ge 39^\circ,\ 1^\circ \le \phi \ge 25^\circ)$, the DEM grid is also resampled to 5' x 5' to meet agreement in resolution with the point within area of computation and the gravity anomalies grid. Since that the data coverage is in a global sense, missing data appears in some regions due to the lack of contrast in the radar image, presence of water, or excessive atmospheric interference. Many global topography datasets have been produced after the appearance of the satellite imagery, this provides better resolution, from 10 arc-minutes (approximately 18 km at the equator) to 30 arc-seconds (approximately 1 km at the Equator) , also filling the large land and marine areas information by using the *US Geological Survey* (USGS) product, GTOPO30. In present study the absolute vertical accuracy of the DEM has been estimated to be 49 m, based on GPS/levelling data.

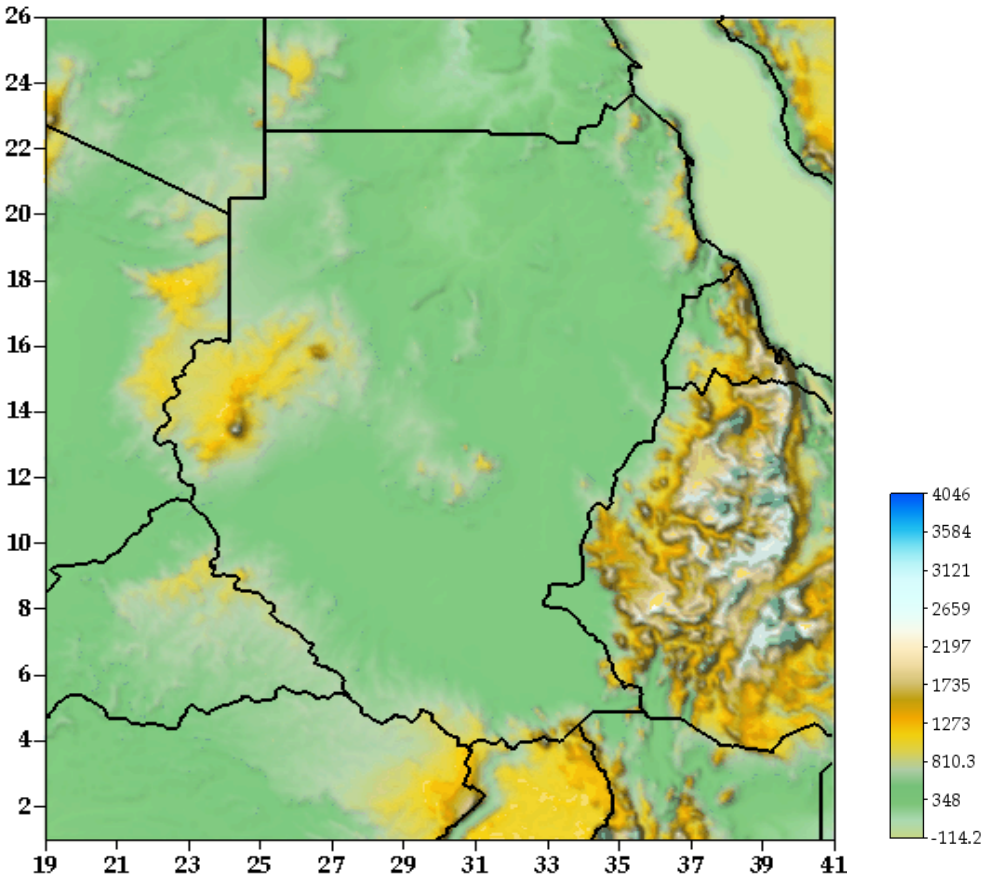

Figure 4.5: SRTM digital elevation model of Sudan.

4.3 The GPS/ levelling data

The GPS/levelling data consists 19 points in Table 4.1 are used in the evaluation and validation of the gravimetric geoid in sense of absolute and relative accuracy. The first geodetic work in Sudan was established in 1903 according to the recommendation of the *International Geodetic Association* (IAG), by continuation of the arc of the 30th meridian from Greece across the African continent starting in Egypt. But actually the work was started in 1935. The Egyptian work was extended until reached to adindan station at northern Sudan. Thereafter, the 30th meridian became the foundation of the geodetic work in Sudan, and the work along continued to the south to the latitude 13' 45" N. The part of 30th meridian next to the latitude 13' 45" N to the boundary with Uganda has been observed with a number of first and second order networks. Between 1961 to 1966 central and north east parts of country were covered. The national reference system in Sudan is based on adindan as planimetric datum and Alexandria (Egypt) as height datum, (Adam M.O 1967).

The levelling data were taken from the old geodetic network and they are varied from 1st to 2nd or 3rd order. The GPS data acquired during different individual projects from 2005 to 2008. The GPS measurements were performed using dual frequency GPS receivers *LEICA 1200*, *LEICA RS500* and *Trimple 5700*, and *choke rings* antennas *ASH701945E_M* from Ashtech, *LEICA AT504*. The antenna height was measured twice in different ways. The measurements were performed twice for a period of 12 hours. GPS/levelling data is one of the constraints for this study because of the difficulties with releasing data. In this study we assume the absolute accuracy if the ellipsoidal and orthometric heights are $\pm 0.05m$ and $\pm 0.1m$ respectively.

Table 4.1: The GPS/levelling data: ellipsoidal, orthometric and derived geoid height used as external measure of the geoid accuracy.

Station	ϕ°	λ°	$h(m)$	$H(m)$	$N_{GPS/levelling}(m)$
GNA	13.42977	22.54811	964.895	954.903	9.992
NYA	12.25005	24.79532	861.938	856.255	5.683
FAR	13.63796	25.27934	1151.618	1143.643	7.975
NHD	12.63172	28.84031	669.853	667.99	1.863
KOO1	8.47061	30.11492	392.98	400.744	-7.764
L460	18.51083	30.63966	681.352	235.359	7.397
L570	19.45993	30.41462	233.68	225.656	8.628
OBD	13.22159	30.43065	242.757	679.443	1.909
JUB	4.92879	31.84812	695.399	707.384	-11.985
MKL	9.40482	32.19385	292.486	297.822	-5.336
L140	19.11531	32.49131	319.008	311.69	7.318
2122	13.40174	33.36026	475.602	477.124	-1.522
2104	14.58145	33.37541	406.613	406.343	0.269
2057	18.49137	33.75019	409.391	402.69	6.7
DMZ	11.79897	34.40649	527.478	530.123	-2.644
QAD	13.46447	35.47824	617.079	618.715	-1.635
HYA	18.32217	36.10055	355.43	351.103	4.327
KAS	15.47695	36.34256	622.469	622.707	-0.238
PRT	18.84264	37.34516	261.159	255.664	5.495

4.4 The Global Gravitational Models (GGMs)

The global gravitational models are representations of the Earth's gravitational potential outside the masses of the Earth in terms of spherical harmonic coefficients. The selection of *global gravitational model* (GGM) in determination of a gravimetric geoid from gravity data can possibly affect the solution, especially when the accuracy is supposed to reach a centimeter level. Four different global gravitational models are tested in this study: EGM96 (combined), EIGEN-GL04C (combined), EIGEN-GRACE02S (satellite-only) and GGM03S (Satellite-only). GGMs are computed and provided by different groups, e.g. GRACE. Accordingly, there are main three classes of GGMs can be summarized as follows.

4.4.1 Satellite-only GGMs

These GGMs are derived from the analysis of the orbits of artificial satellites, known by satellite tracking. These models were limited in precision in the past because of: the combined impact of high attitude of satellites, incomplete tracking of satellite orbits from the ground stations; inaccurate modeling of atmospheric drag; non-gravitational perturbations; and incomplete sampling of the global gravity field. Recently, most of accuracy limitations have been reduced significantly by using the dedicated satellite gravimetry missions CHAMP and GRACE, Rummel *et al*. (2002) and Featherstone (2002a). In this study two combined GGMs were used EIGEN-GRACE02S and GGM03S.

4.4.2 Combined GGMs

The GGMs are derived from the combination of satellite data, land and ship track gravity observations, and marine airborne gravity data (e.g., Rapp, 1997b). Due to this combination we find that the some combined GGMs have higher harmonic degrees. In addition to the above limitations of satellite-only GGMs, spatial coverage of the terrestrial data also has an influence on combined GGMs accuracy. The long-wavelength component in terrestrial gravity anomalies suffer from distortions and offsets between different vertical datums (e.g. Heck, 1990). In this study two combined GGMs were used, EGM96 complete to degree and order 360 and EIGEN-GL04C complete to degree and order 360 as well.

4.4.3 Tailored GGMs

The tailored GGMs are derived from an adjustment of existing *(satellite or combined)* GGMs using higher resolution gravity data that may have not necessarily have been used previously (e.g. Wenzel, 1998a, 1998b). This can be obtained by deriving corrections of the gravitational coefficients from integral formulas. Tailored GGMs should be applied only over the area which the tailoring was applied in order to avoid effects appear on areas without data. In our study tailored GGMs have not been used.

4.4.4 EGM96

For about three years the *National Aeronautics and Space Administration* (NASA), the *National Imagery and Mapping Agency* (NIMA) and the Ohio State University worked uniquely to

determine an improved spherical harmonic model of the Earth to degree and order 360. The model is EGM96, which is a composite solution that consists of a combination solution to degree and order 70, a block diagonal solution from degree 71 to 359, and a quadrature solution at degree 360. The combination model comprises satellite tracking data to over 20 satellites, including those tracked by *Satellite Laser Ranging* (SLR) 18 satellites, GPS, the *Tracking Data Relay Satellite System* (TDRSS) and Tranet Doppler, direct altimetry from TOPEX, ERS-1, and GEOSAT and in addition the normal equations of the 1°x1° surface gravity data (without the altimeter derived anomalies) to degree and order 70. These satellites were chosen to be from a wide range altitude and inclination to sample the geoptential orbital perturbations over a variety of frequencies. The quadrature solution is based on the satellite only counterpart of EGM96 (EGM96S) beside the surface gravity data and altimeter derived anomalies. The block diagonal solution is also built on EGM96S; it uses the same resolution data (30'x30') and taking the quadrature solution as a reference. The error covariance is complete to degree and order 70; the coefficient standard deviations only are available from degree 71 to degree 360. EGM96 utilized surface gravity data from different region of the globe comprising data recent released from the NIMA archives. The collection of terrestrial gravity data by NIMA contains airborne gravity surveys over Greenland and parts of the Arctic and the Antarctic, surveyed by the *Naval Research Lab* (NRL) in addition to collection projects conducted by the University of Leeds have improved the data holdings over many of the world's land areas. EGM96 represents a major advance in the modeling of the Earth's geoid in both land and ocean areas.

4.4.5 EIGEN-GL04C

The combined gravitational model EIGEN-GL04C was released on March 31, 2006; it is an upgrade of EIGEN-CG03C. It is a combination GRACE and LAGEOS mission with high resolution 0.5° x 0.5° gravimetry and altimetry surface data. The satellite data have been analyzed by GFZ Potsdam and GRGS Toulouse. All surface gravity data are alike those of EIGEN-CG03C excluding the geoid undulations over the oceans derived from a new GFZ *mean sea surface height* (MSSH) model minus the ECCO sea surface topography (EIGEN-CG03C: CLS01 MSSH minus ECCO). EIGEN-GL04C is complete to degree and order 360 in terms of spherical harmonic coefficients and thus resolves geoid and gravity anomaly wavelengths of 110 km. High-resolution combination gravity models are important for all

applications that require precise knowledge of the static gravity potential and its gradients are needed in the medium and short wavelength spectrum. EIGEN-GL04S1 represents the satellite-only part of EIGEN-GL04C; this part can be derived by reduction of the terrestrial normal equation system and is complete up to degree and order 150.

4.4.6 EIGEN-GRACE02S

EIGEN-GRACE02S is a medium-wavelength gravity field model which is calculated from 110 days of GRACE tracking data and was released on February 13, 2004. The EIGEN-GRACE02S solution resulting from the least-squares adjustment has been derived only from GRACE intersatellite observations and is independent from oceanic and continental surface gravity data. This model that resolves the geoid with on accuracy of better than 1 *mm* at a resolution of 1000 km half-wavelength is about one order of magnitude more accurate than recent CHAMP derived global gravity models and more than two orders of magnitude more accurate than the latest pre-CHAMP satellite-only gravity models and it provides full power almost up to degree 120.

4.4.7 GGM03S

A new generation Earth gravitational field model GGM03S, recently released, is derived using four years of data spanning January 2003 to December 2006 from GRACE. Since release of GGM02, there have been improvements in data-products and gravity estimation methods in both these forms: GGM02S - complete to harmonic degree 160 is derived purely from GRACE satellite data, and is unconstrained by any other information; and GGM02C (combined model) complete to degree 200. GGM03S complete to harmonic degree 180, based on the calibrated covariance, GGM03S represents a factor of two improvements over the previous GGM02 model. In this study the GGM03S has been used up to degree of 120.

4.4.8 EGM2008

The Earth Gravitational Model EGM2008 has been publicly released by the National Geospatial-Intelligence Agency (NGA) EGM Development Team. This gravitational model is complete to spherical harmonic degree and order 2159, and contains additional coefficients extending to degree 2190 and order 2159. EGM2008 includes improved 5′ x 5′ minute gravity

4.4.8. EGM2008

anomalies and has been enhanced from the latest GRACE based satellite solutions. EGM2008 also includes improved altimetry-derived gravity anomalies estimated using PGM2007B and its implied Dynamic Ocean Topography (DOT) model as reference. For the Collocation prediction of the final 5' x 5' mean gravity anomalies, PGM2007B is used as reference model, and employed a formulation that predicts area-mean gravity anomalies which are effectively band limited; this model has not been used in this study.

Chapter 5

Geoid height computation

In this chapter we are going to show relevant studies in Sudan and verify the new gravimetric geoid model on the Earth by using GPS/levelling data. As mentioned in Chapter 4, the wide use of GPS needs high-resolution geoid models to convert the ellipsoidal heights h provided by GPS into orthometric heights to be used in compatible way with those on the local vertical datum. The accuracy of a gravimetric geoid can be estimated internally by the expected global mean square error of Least-squares method, externally by verifying gravimetric geoid height with derived geoid heights from GPS/levelling data in absolute and relative senses.

5.1 Relevant geoid studies in Sudan

In 1967, the first attempt to compute a geoid was done by (Adam M.O 1967), Cornell University, USA, he used 46 astrogeodetic stations to compute deflections of vertical ξ, η and separation between the geoid and the reference ellipsoid (Clarke 1880). Due to lack of data from neighboring countries and large un-surveyed areas in Northwest and Southwest parts of Sudan, Adam found that the information was insufficient to determine the accurate geoid in Sudan and recommended to fill all gabs over there.

Another study was conducted by Fashir (1991), to compute a gravimetric model of Sudan by using heterogeneous data. Fashir's model was computed to cover a grid of $(5^\circ \le \phi \le 22^\circ,\ 22^\circ \le \lambda \le 38^\circ)$ referred to the geodetic reference system 1980 (GRS80) transformed to the local datum (Adindan Datum). Fashir (1991) used modified Stokes' kernel and *Goddard Earth Model* (GEM-T1) geoptential model, direct and indirect of atmospheric and topographic attractions effect was examined as well as ellipsoidal effect on the computed geoid.

5.2 Practical evaluation of the integral (Stokes') formula

5.2. Practical evaluation of the integral (Stokes') formula

The integral formula can be evaluated approximately by summation. The surface elements $d\sigma$ are replaced by small but finite compartments q which can be obtained by a subdividing of the surface of the Earth suitably by using two different methods the *grid lines method* or the *template method*. The *template method* is easy to be used for theoretical considerations applying polar coordinates (ψ,α), while the *grid method* using geodetic coordinates (ϕ,λ) and is most suitable for computer programming, therefore it has been selected in this study.

In grid lines method, the subdivision can be achieved by the grid lines of some fixed coordinates system (ϕ,λ) forming either rectangular or square blocks. Therefore the first term of the modified formula can be evaluated numerically by:

$$\left.\begin{aligned}
\tilde{N}_1 &= \frac{c}{2\pi}\iint_{\sigma_o}\Delta g\, S^L(\psi)\, d\sigma = \frac{c}{2\pi}\sum_i\sum_j\iint_{\sigma_{ij}}\Delta g\, S^L(\psi)\, d\sigma_{ij} \\
&\approx \frac{c}{2\pi}\sum_i\sum_j\iint_{\sigma_{ij}}\Delta\bar{g}_{ij}\, S^L(\psi_{ij})\, d\sigma_{ij} = \frac{c}{2\pi}\sum_i\sum_j\Delta\bar{g}_{ij}\, S^L(\psi_{ij})\iint_{\sigma_{ij}} d\sigma_{ij} \\
&= \frac{c}{2\pi}\sum_i\sum_j\Delta\bar{g}_{ij}\, S^L(\psi_{ij})\iint_{\sigma_{ij}} d\sigma_{ij} \\
&= \frac{c}{2\pi}\sum_i\sum_j\Delta\bar{g}_{ij}\, S^L(\psi_{ij})\, A_{ij}
\end{aligned}\right\}, \qquad (5.1)$$

where ψ_{ij} is the spherical distance from the computation point (ϕ,λ) to the block center of σ_{ij} and A_{ij} is the area of the block σ_{ij}. The spherical distance ψ_{ij} can be computed by the following formula:

$$\cos\psi_{ij} = \sin\phi\sin\phi_i + \cos\phi\cos\phi_i\cos\left(\lambda-\lambda_j\right), \qquad (5.2)$$

$$\phi_i = \phi_{\min} + (i-\frac{1}{2})\Delta\phi, \qquad (5.3)$$

$$\lambda_i = \lambda_{\min} + (i-\frac{1}{2})\Delta\lambda, \qquad (5.4)$$

where (ϕ,λ) and (ϕ_i,λ_j) are the latitude and the longitude of the computation point and the block center respectively. The area of each block A_{ij} can be computed as follows:

$$A_{ij} = \iint_{\sigma_{ij}} d\sigma = 2\Delta\lambda \sin\left(\Delta\phi/2\right)\cos\phi_i, \tag{5.5}$$

Figure 5.1 shows equi-angular blocks 5′ x 5′ formed by the geodetic coordinates (ϕ, λ), inside the target area of computation, subdivided surface area of the computation.

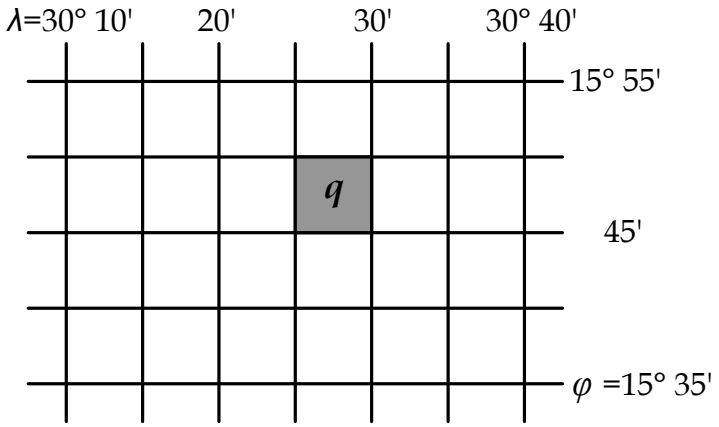

Figure 5.1: Grid lines with equi-angular blocks 5′ x 5′.

5.3 Solving the least-squares modification parameters

In this study least-squares coefficients has been computed using a special software **LS_coeff.m** designed by Dr. Artu Ellmann. The software consists of seven computational sub-routines: **sigma_terr_1.m, ggm_degree_variances_2.m, trunc_coeff_3.m, tsvd_4.m, ttls_5.m, BN_boeff_plot_6.m, modif_kernel_7.m.** These subroutines are connected with the master-routine **LS_coeff.m.** The numbers attached in sub-routine names indicate the calling order. The software overcomes certain difficulties of solving the modification parameters from the system of linear equations, especially the design matrix in unbiased and optimum LSM which suffer from *ill-conditioning* or instability. In general, the matrix becomes *ill-conditioned* when the outcome result affected extremely by the changes happened to the coefficients of the solution. This possibly alters the iterative solver to be a tricky operation due to the matrix singular status. Hence, the regular matrix inverse cannot be computed normally as before, which leads to a great amplification on noisy elements and rounding errors during the inversion process. The condition number of a matrix is an indication of the *ill-condition* of the matrix and can be found using the matrix e.g. $\mathbf{A}$ and its inversion $\mathbf{A}^{-1}$.

5.3.1. Modification limits

When the condition number (cond (**A**)) is bigger, **A** becomes more *ill-conditioned*. Normally, well-conditioned matrices have small condition numbers. The solution of *ill-conditioning* is to include some regularization techniques so as to re-standardize the matrix. Two simple regularization methods *Truncated Singular Value Decomposition* (T-SVD) and *Truncated Total Least Squares* (T-TLS) were used by Ellmann (2005) in **LS_coeff.m** software, to gain a meaningful solution for the *ill-condition* problem. After the LS coefficients s_n and b_n are obtained, they are used in our computations to compute an approximate geoid height and additive corrections except the topographic correction where s_n and b_n are not needed.

5.3.1 Modification limits

The modifying of Stokes' formula is mainly aiming to minimize the truncation error, whereas the integration cap around the computation point is often limited to a few hundred kilometers, due to the lack of terrestrial gravity data coverage. Hence the selection of the upper limit M of the GGMs and the upper bound of the harmonics to be modified in Stokes' function, L are extremely essential in geoid modeling to increase the computational efficiency. This means using higher degree GGMs may significantly compensate the shortage of gravity data. On the contrary, error stemming from potential coefficients increases proportionally with increasing in GGMs degree. Therefore an equalized point between the GGM and the terrestrial gravity data should be found throughout many arguments. Three LSM methods, biased (Sjöberg, 1984), unbiased (Sjöberg, 1991) and optimum (Sjöberg, 2003) are tested in this study to achieve the final geoid model of Sudan. These methods assumed that the upper limit of modification L is at least as high as M, i.e. $L \geq M$. In this study, $L = M$ is considered to test the potential of the 4 GGMs.

The master program **LS.coeff.m** admits the user to set the characteristics of data (initial conditions), the area of computation and other modification features. The condition number of the **A** matrix (cond (**A**)) for the biased method is less than 10^3, while for the other two methods ranges from 10^{15} to 10^{18}. The system equation for the biased method is comparably *well-conditioned.* This means that it is able to be solved regularly by inversing **A** matrix. On the other hand, unbiased and optimum methods have *ill-conditioned* systems and the parameters s_n had oscillation up to range $\pm 10^5$.

With the same initial conditions $(C(0), M, L \text{ and } \psi_\circ)$ input by the user, very similar parameters b_n have been obtained for the three methods. The unbiased/optimum parameters solved by the regularization should not deviate more than 10^{-2} from the biased parameters. Meanwhile, the residual norm ($\|\mathbf{As-h}\|_2$) of the final parameters should remain less than 10^{-12} when used in geoid determination. In this study, satisfactory results of least-squares modification parameters have been accomplished within the given tolerance. Tables 5.1, 5.2 and 5.3 show the effect of using different GGMs, different cap sizes and different values for terrestrial gravity anomalies error. In this study four GGMs with their full effective degree and order, were tested with the same cap size $\psi_\circ$ and $\sigma_{\Delta g}$ in Table 5.1. All given results are after fitting with 7-Parameter model.

Table 5.1: Testing 4 different GGMs with their full degree with the same cap size $\psi_\circ$ and gravity data $\sigma_{\Delta g}$ versus 19 GPS/levelling data, in order to select the best GGM which gives best improvement after fitting.

$\psi_\circ = 3^\circ,\ \sigma_{\Delta g} = 9$				
GGM	EIGEN-GL04C (SGA)	EGM96 (SGA)	EIGEN-GRACE02S (S)	GGM03S (S)
M=L	360	360	120	120
LSM	Biased	Optimum	Optimum	Biased
σ	0.32	1.1	**0.29**	0.522

From Tables 5.1, 5.2 and 5.3 we can see that EIGEN-GRACE02S (satellite-only) and EIGEN-GL04C (combined model) give the best and the same fitting level than others models. In Table 5.2 we estimated 3 different priori values ($\sigma_{\Delta g} = 1,\ 4 \text{ and } 9$ *mGal*^{2}) for the accuracy of the gravity data to find out better result versus GPS/levelling data. 9 mGal^2 gives the best result in the optimum solution of the LSM, EIGEN-GRACE02S up to degree of 120, and cape size $\psi_\circ = 3^\circ$. In Table 5.3 different values of the cape size $\psi_\circ$ were tested and compared in the LSM with 120 degree of EIGEN-GRACE02S and the cape size $\psi_\circ = 3^\circ$ and 9 mGal^2 as the accuracy of the gravity data.

5.3.1. Modification limits

Table 5.2: Pre-estimated values of accuracies for the gravity data $\sigma_{\Delta g}$, the degree of EIGEN-GRACE02S (satellite-only) is up to 120.

GGM: EIGEN-GRACE02S, $\psi_\circ = 3^\circ$, $M = L = 120$			
$\sigma_{\Delta g}(mGal)$	1	4	9
LSM	Optimum	Optimum, unbiased and biased	Optimum
σ	0.384	0.354	**0.29**

Table 5.3: Testing different values of the cape size $\psi_\circ$ in LSM, accuracy of the gravity data $\sigma_{\Delta g} = 9$ and the degree of EIGEN-GRACE02S (satellite-only) is up to 120.

GGM: GRACE02S, $\sigma_{\Delta g} = 9$, M=L=120			
$\psi_\circ$	1°	3°	5°
LSM	Optimum	Optimum	Biased
σ	0.423	**0.29**	0.432

In current study, the based on result from above tables, we considered the accuracy of the gravity data as $\sigma_{\Delta g} = 9\ mGal^2$.

5.4 External accuracy of the gravimetric geoid model

GPS/levelling data commonly used to verify gravimetric geoid, height given by GPS, is the ellipsoidal height h based on WGS84 reference ellipsoid, while the orthometric height H is given by Spirit-levelling. Orthometric heights subtracted from ellipsoidal heights algebraically to give heights N can be used as evaluation of a gravimetric geoid models. The fundamental expression of relationship between h, H and N is given by:

$$h \approx H + N \tag{5.6}$$

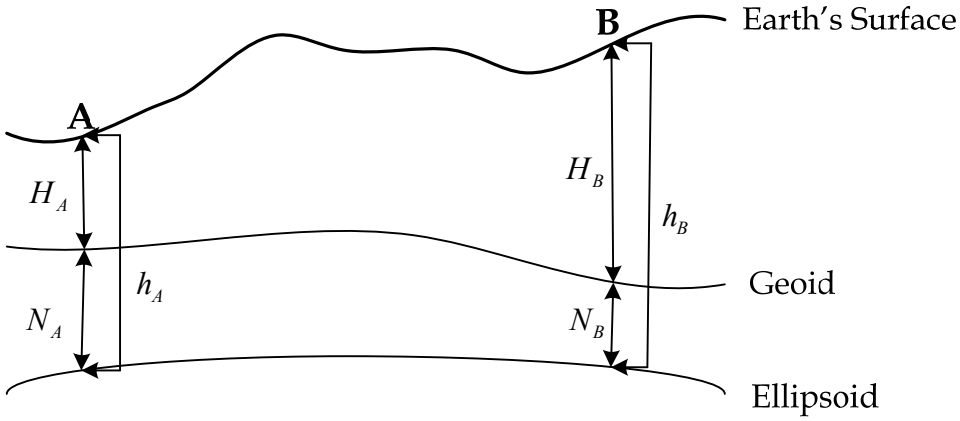

Figure 5.2: Relationship between ellipsoidal, orthometric and geoid height

In Equation (5.6), the approximate equality is due to the torsion of the plumb line and the deflection of vertical, which is more affective to the approximation. The approximation error can be estimated by multiplying orthometric height with cosine of deflection of vertical, however, in this study it is not considered. Moreover, GPS, orthometric and geoid heights have their own error budgets of random and systematic errors e.g., Long-wavelength errors from the gravitational model used, short-wavelength error from the digital terrain model, biases in gravity anomaly due to inconsistencies of gravity datum, vertical and horizontal datum inconsistencies (offsets and distortions), as well as systematic distortions and short-wavelength errors caused by theoretical assumptions made in computation of the vertical gravity gradient affect the geoid N and consequently, the approximation in Equation (5.6).

5.4. External accuarcy of the gravimetric geoid model

Table 5.4: 19 GPS/levelling points with, ellipsoidal heights, orthometric heights and derived geoid heights from GPS/levelling data.

Station	ϕ°	λ°	h (m)	H (m)	$N_{GPS/levelling}$ (m)
GNA	13.42977	22.54811	964.895	954.903	9.992
NYA	12.25005	24.79532	861.938	856.255	5.683
FAR	13.63796	25.27934	1151.618	1143.643	7.975
NHD	12.63172	28.84031	669.853	667.99	1.863
KOO1	8.47061	30.11492	392.98	400.744	-7.764
L460	18.51083	30.63966	681.352	235.359	7.397
L570	19.45993	30.41462	233.68	225.656	8.628
OBD	13.22159	30.43065	242.757	679.443	1.909
JUB	4.92879	31.84812	695.399	707.384	-11.985
MKL	9.40482	32.19385	292.486	297.822	-5.336
L140	19.11531	32.49131	319.008	311.69	7.318
2122	13.40174	33.36026	475.602	477.124	-1.522
2104	14.58145	33.37541	406.613	406.343	0.269
2057	18.49137	33.75019	409.391	402.69	6.7
DMZ	11.79897	34.40649	527.478	530.123	-2.644
QAD	13.46447	35.47824	617.079	618.715	-1.635
HYA	18.32217	36.10055	355.43	351.103	4.327
KAS	15.47695	36.34256	622.469	622.707	-0.238
PRT	18.84264	37.34516	261.159	255.664	5.495

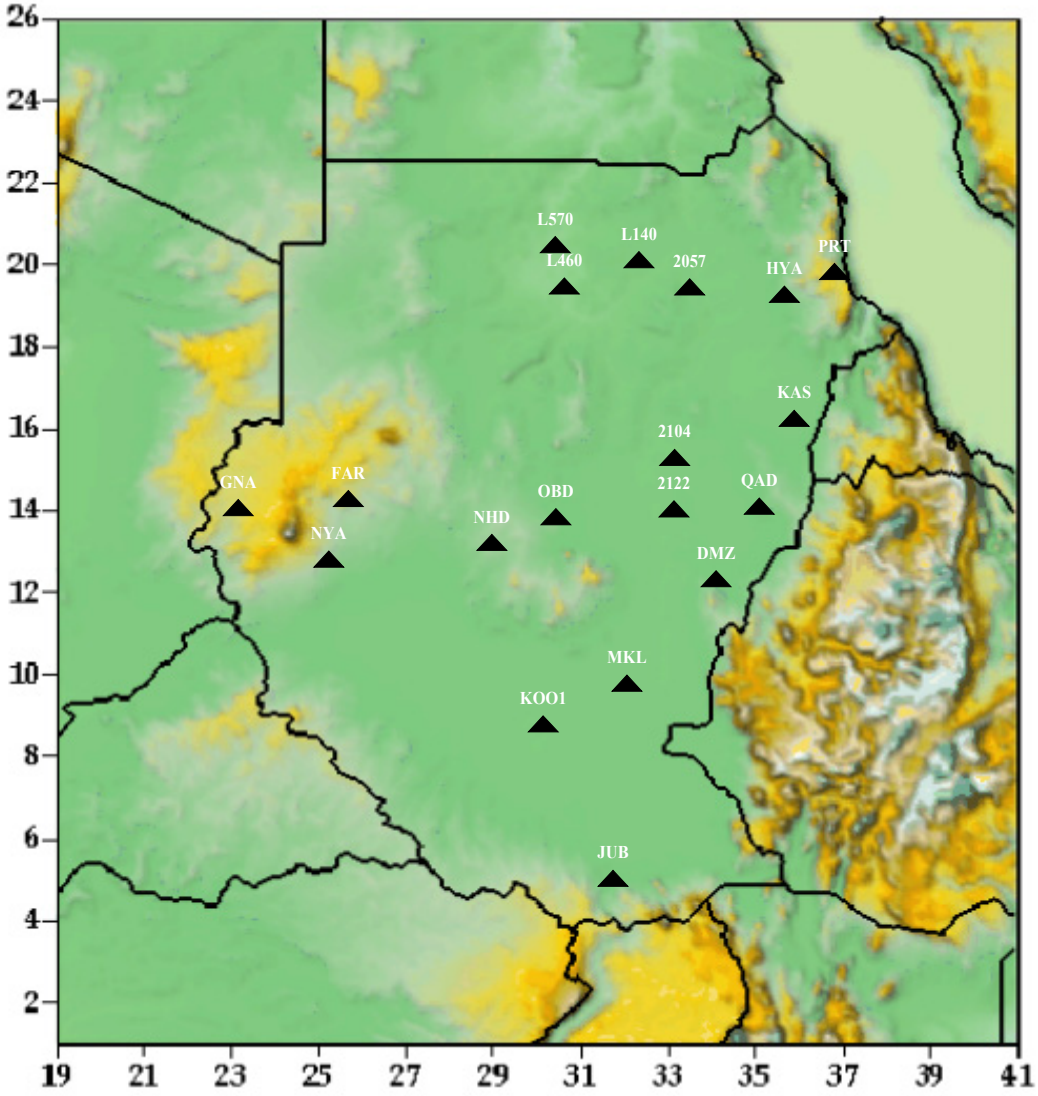

Figure 5.3: Distribution of GPS/levelling points inside Sudan.

5.4.1 Verification of the geoid in absolute sense

Systematic errors, distortions and datum inconsistencies between orthometric, ellipsoidal and geoid height can be absorbed by fitting GPS/levelling derived geoid height to a gravimetric geoid height using least-squares adjustment and using several models, four, five and seven parameter model.

$$\Delta N_i = N_i^{GPS} - N_i = h_i - H_i - N_i = \boldsymbol{a}_i^T \mathbf{x} + \boldsymbol{\varepsilon}_i \tag{5.7}$$

where N_i is the interpolated geoidal height value for the i GPS point, considering points from the geoid model that exist in the neighborhood, $\mathbf{x}$ is a $n \times 1$ vector of unknown parameters (where n the number of the GPS/levelling points), $\boldsymbol{a}_i$ is a $n \times 1$ vector of known coefficients, and ε_i denotes a residual random noise term. The parametric model $\boldsymbol{a}_i^T \mathbf{x}$ is supposed to describe the mentioned systematic errors and inconsistencies inherent in the different height data sets. The models tested in this study are:

4-Parameter model:

$$\boldsymbol{a}_i = (\cos\phi_i \cos\lambda_i \quad \cos\phi_i \sin\lambda_i \quad \sin\phi_i \quad 1)^T \text{ and } \mathbf{x} = (x_1 \quad x_2 \quad x_3 \quad x_4)^T, \tag{5.8}$$

5-Parameter model:

$$\boldsymbol{a}_i = (\cos\phi_i \cos\lambda_i \quad \cos\phi_i \sin\lambda_i \quad \sin\phi_i \quad 1 \quad \sin^2\phi_i)^T \text{ and } x = (x_1 \quad x_2 \quad x_3 \quad x_4 \quad x_5)^T, \tag{5.9}$$

7-Parameter model:

$$\boldsymbol{a}_i = \begin{pmatrix} \cos\phi_i \cos\lambda_i \\ \cos\phi_i \sin\lambda_i \\ \sin\phi_i \\ \cos\phi_i \sin\phi_i \cos\lambda_i / W_i \\ \cos\phi_i \sin\phi_i \sin\lambda_i / W_i \\ \sin^2\phi_i / W_i \\ 1 \end{pmatrix} \quad \textit{and} \quad \mathbf{x} = \begin{pmatrix} x_1 \\ x_2 \\ x_3 \\ x_4 \\ x_5 \\ x_6 \\ x_7 \end{pmatrix}, \tag{5.10}$$

where (ϕ, λ) the horizontal geodetic coordinates of the GPS/levelling points and,

$$W_i = \left(1 - e^2 \sin^2 \phi_i\right)^{1/2} , \tag{5.11}$$

where *e* is the first eccentricity of the reference ellipsoid. We then obtain the following matrix system of observation equations:

$$\mathbf{Ax} = \mathbf{\Delta N} - \boldsymbol{\varepsilon} , \tag{5.12}$$

where $\mathbf{A}$ is the design matrix composed of one row $\boldsymbol{a}_i^T$ for each observation ΔN_i. The least-squares adjustment to this equation utilizing the mean squares of the residuals ε_i becomes:

$$\hat{\mathbf{x}} = \left(\mathbf{A}^{\mathbf{T}}\mathbf{A}\right)^{-1} \mathbf{A}^{\mathbf{T}}\mathbf{\Delta N}, \tag{5.13}$$

Yielding the residuals

$$\hat{\boldsymbol{\varepsilon}} = \mathbf{\Delta N} - \mathbf{A}\hat{\mathbf{x}} = \left[\mathbf{I} - \left(\mathbf{A}^{\mathbf{T}}\mathbf{A}\right)^{-1} \mathbf{A}^{\mathbf{T}}\right]\mathbf{\Delta N}, \tag{5.14}$$

The variance-covariance matrices of the estimated parameters $\hat{\mathbf{x}}$ and $\hat{\boldsymbol{\varepsilon}}$ are as follow:

$$\begin{aligned} \mathbf{C}_{\mathbf{xx}} &= \sigma_\circ^2 (\mathbf{A}^{\mathbf{T}}\mathbf{A})^{-1} \\ \mathbf{C}_{\hat{\boldsymbol{\varepsilon}}\hat{\boldsymbol{\varepsilon}}} &= \sigma_\circ^2 \left[\mathbf{I} - \left(\mathbf{A}^{\mathbf{T}}\mathbf{A}\right)^{-1} \mathbf{A}^{\mathbf{T}}\right] \end{aligned} \tag{5.15}$$

where $\sigma_\circ$ is the variance factor can be estimated from the residuals $\hat{\boldsymbol{\varepsilon}}$:

$$\sigma_\circ = \sqrt{\frac{\hat{\boldsymbol{\varepsilon}}^{\mathbf{T}}\hat{\boldsymbol{\varepsilon}}}{n-m}}, \tag{5.16}$$

where *n* is the number of GPS/levelling points and *m* is the number of estimated parameters.

The main problem of using these models is that the final residuals $\hat{\varepsilon}$ hold a combined amount of random errors related to GPS, levelling and Geoid. Therefore this absolute verification does not show the real potential of the geoid models, so the final residuals are not the exact error of the gravimetric geoid model. The standard devia-

5.4.1. Verification of the geoid in absolute sense

tion of the residuals $\hat{\varepsilon}$ after fitting is taken as an indication of the absolute accuracy of the geoid model.

Table 5.5: Differences between the approximate geoid heights (before adding the additive corrections) and the derived geoid heights from GPS/levelling data. With contribution of EIGEN-GRACE02S and EIGEN-GL04C.

Station	EIGEN-GRACE02S		EIGEN-GL04C	
	Before fitting	After fitting	Before fitting	After fitting
	ΔN (m)	*ε (m)*	*ΔN (m)*	*ε (m)*
GNA	1.306	-0.073	1.464	-0.259
NYA	1.268	0.112	1.529	0.297
FAR	0.933	0.095	1.187	0.208
NHD	0.815	0.204	0.480	0.003
KOO1	0.205	-0.875	0.201	-0.757
L460	-0.605	-0.561	-0.124	-0.302
L570	-0.182	-0.092	0.311	-0.044
OBD	0.928	0.469	0.694	0.451
JUB	1.397	0.190	1.240	0.152
MKL	1.221	0.354	1.010	0.347
L140	0.206	0.140	0.149	-0.111
2122	0.440	-0.046	-0.122	-0.244
2104	0.142	-0.244	-0.181	-0.216
2057	0.908	0.687	0.903	0.684
DMZ	0.700	0.019	0.387	0.086
QAD	1.002	0.348	0.451	0.250
HYA	0.072	-0.536	-0.163	-0.653
KAS	0.036	-0.644	-0.134	-0.382
PRT	1.349	0.452	1.346	0.490
σ	0.589	0.416	0.599	0.386

As we can see from Table 5.5 the gravitational models EIGEN-GRACE02S and EIGEN-GL04C are corresponding closely by having nearly standard deviations of the residuals before and after fitting. A considerable enhancement in the standard deviations of the approximate geoid height residuals without the additive corrections and after applying the 7-parameter model appears clearly. EIGEN-GRACE02S (satellite only) was chosen for the

final computations of the new geoid model of Sudan (KTH-SDG08).

Table 5.6: Differences between the derived geoid heights from GPS/levelling data and the gravimetric geoid heights before and after 4-Parameter, 5-Parameter and 7-Parameter fitting with contribution of EIGEN-GRACE02S.

Station	Before fitting	After fitting		
	ΔN (m)	7-Parameter	5-Parameter	4-Parameter
		ε (m)	ε (m)	ε (m)
GNA	2.094	0.059	-0.172	0.074
NYA	2.011	-0.169	0.026	0.126
FAR	1.831	0.099	0.049	0.113
NHD	1.962	0.172	0.408	0.379
KOO1	2.391	-0.243	0.427	0.331
L460	0.367	-0.419	-0.685	-0.878
L570	0.823	-0.046	-0.178	-0.426
OBD	1.801	0.263	0.344	0.313
JUB	2.093	0.082	-0.332	-0.587
MKL	2.171	-0.026	0.288	0.262
L140	1.146	0.084	0.086	-0.097
2122	1.325	-0.074	-0.208	-0.158
2104	1.032	-0.182	-0.397	-0.366
2057	1.815	0.638	0.643	0.546
DMZ	1.558	-0.032	-0.217	-0.108
QAD	1.788	0.422	0.058	0.229
HYA	1.138	-0.517	-0.293	-0.235
KAS	0.962	-0.396	-0.707	-0.513
PRT	2.449	0.286	0.863	0.995
σ	0.576	**0.29**	0.421	0.447

In current study and from Table 5.6, 7- Parameter model (Kotsakis and Sideris 1999) gives the best fitting residuals with minimum standard deviation 0.29 *m* comparing to 5-Parameter and 4-Parameter 0.42 *m* and 0.45 *m* respectively**.** Table 5.7 shows the statistical analysis of the residuals after fitting with minimum, maximum, mean, root mean squares and standard deviation of the residuals after fitting.

5.4.1. Verification of the geoid in absolute sense

Table 5.7: Statistical analysis of absolute accuracy of Sudan geoid versus 19 GPS/levelling data.

	Before fitting	**After fitting**		
	ΔN (m)	7-Parameter	5-Parameter	4-Parameter
		ε (m)	*ε (m)*	*ε (m)*
min	0.367	-0.517	-0.707	-0.878
max	2.449	0.638	0.863	0.995
mean	1.619	0.000	0.000	0.000
σ	0.576	**0.29**	0.421	0.447

The residuals which are given by the 7-Parameter model are corresponding closely to zero value than the other two models. Figure 5.4 illustrates residuals plot of 7-Parameter model, 5- and 4-Parameter.

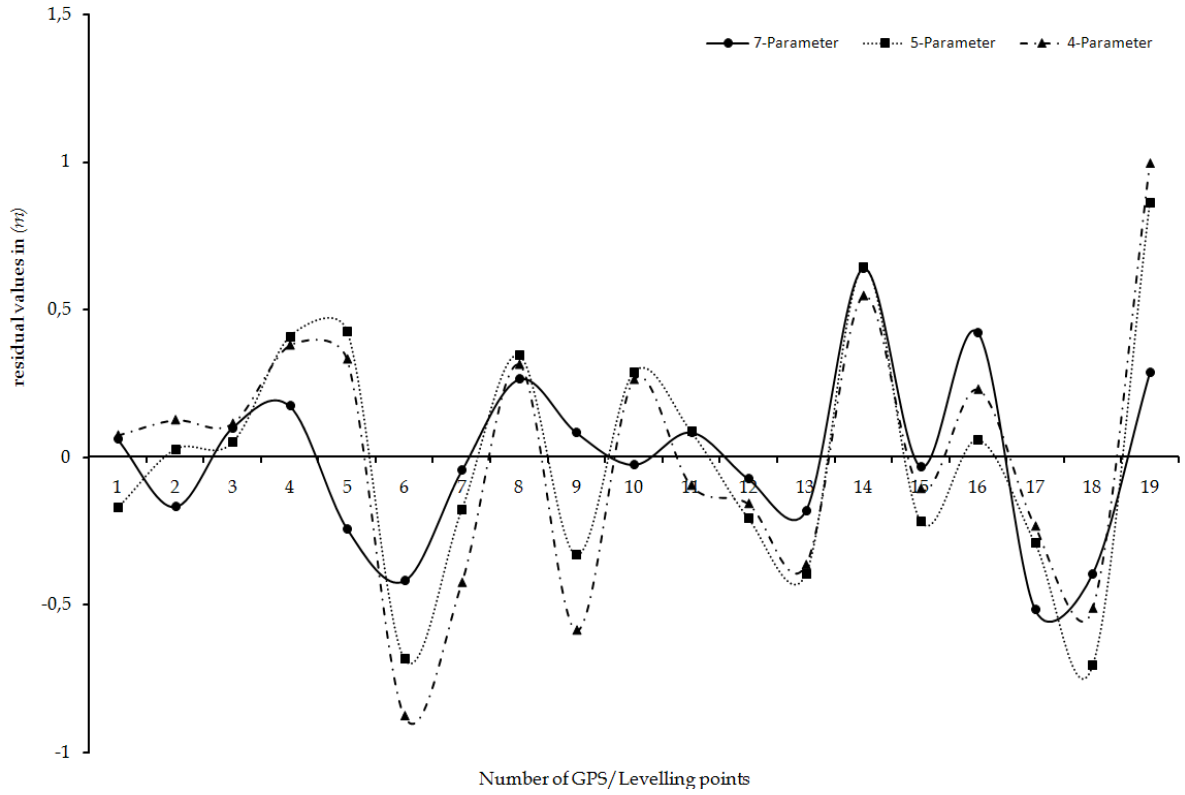

Figure 5.4: Residuals of the 7, 5 and 4-Parameter models in blue, red and green, respectively.

Table 5.8: Values of 4- Parameter , 3 translations and 1 scale factor, with their standard deviations.

Parameter	Value	σ_{x_i}
x_1	-39.1505	14.60947
x_2	-24.1078	8.682276
x_3	-15.763	4.200633
x_4	49.84208	17.38357

Table 5.9: Values of 5- Parameter , 3 translations, 1 rotation and 1 scale factor, with their standard deviations.

Parameter	Value	σ_{x_i}
x_1	-73.6058	18.71775
x_2	-43.6057	10.88979
x_3	-8.69372	4.756108
x_4	88.66236	21.75203
x_5	-36.9433	13.40677

Table 5.10: Values of 7- Parameter , 3 translations, 3 rotations and 1 scale factor, with their standard deviation.

Parameter	Value	σ_{x_i}
x_1	214.6487	38.57145
x_2	103.1723	24.81921
x_3	1195.279	211.4433
x_4	-1010.28	165.4852
x_5	-506.927	111.0021
x_6	-256.785	44.66376
x_7	-238.331	46.36037

In consonance with the numerical results of these three models showed in the above Tables 5.8, 5.9 and 5.10 as well as Figure 5.4. It is found that the 7-Parameter model provides a meaningful augmentation in the residuals standard deviation after fitting and it has also significant estimated parameters when compared to their standard errors. The parameters

5.4.1. Verification of the geoid in absolute sense

are used to convert the geoid model into the geometrical geoid. Due to the fact that some of the collected data are affected by long-wavelength errors, therefore it is important to mention that these parameters do not represent the actual datum shift parameters e.g. translation, rotation and scale factor. Figure 5.5 shows that the standard error of the each estimated residuals by the 7-Parameter model is the minimum, comparing with 4 and 5-Parameter models.

Table 5.11: The derived geoid heights from GPS/levelling data and the corrected gravimetric geoid heights computed by choosing EIGEN-GRACE02S gravitational model in the combined method, columns 6 shows the differences between the derived geoid heights and the gravimetric geoid heights before fitting while column 7 shows the residuals after 7-Parameter fitting.

Station	ϕ°	λ°	$N_{GPS/levelling}$ *(m)*	$N_{corrected}$ *(m)*	**EIGEN-GRACE02S**	
					Before fitting	After fitting
					ΔN *(m)*	ε *(m)*
GNA	13.42977	22.54811	9.992	7.898	2.094	0.059
NYA	12.25005	24.79532	5.683	3.672	2.011	-0.169
FAR	13.63796	25.27934	7.975	6.144	1.831	0.099
NHD	12.63172	28.84031	1.863	-0.099	1.962	0.172
KOO1	8.47061	30.11492	-7.764	-10.155	2.391	-0.243
L460	18.51083	30.63966	7.397	7.03	0.367	-0.419
L570	19.45993	30.41462	8.628	7.805	0.823	-0.046
OBD	13.22159	30.43065	1.909	0.108	1.801	0.263
JUB	4.92879	31.84812	-11.985	-14.078	2.093	0.082
MKL	9.40482	32.19385	-5.336	-7.507	2.171	-0.026
L140	19.11531	32.49131	7.318	6.172	1.146	0.084
2122	13.40174	33.36026	-1.522	-2.847	1.325	-0.074
2104	14.58145	33.37541	0.269	-0.763	1.032	-0.182
2057	18.49137	33.75019	6.7	4.885	1.815	0.638
DMZ	11.79897	34.40649	-2.644	-4.202	1.558	-0.032
QAD	13.46447	35.47824	-1.635	-3.423	1.788	0.422
HYA	18.32217	36.10055	4.327	3.189	1.138	-0.517
KAS	15.47695	36.34256	-0.238	-1.2	0.962	-0.396
PRT	18.84264	37.34516	5.495	3.046	2.449	0.286
				σ	0.576	**0.29**

Referring to Tables 5.5 and 5.11 we notice that there is a significant improvement by adding the additive corrections to the approximate geoid. The additive corrections have improved the standard deviation of the final gravimetric geoid height after using 7-Parameter fitting to become $\pm 0.29\ m$ instead of $\pm 0.42\ m$ in the approximate geoid heights (without additive corrections).

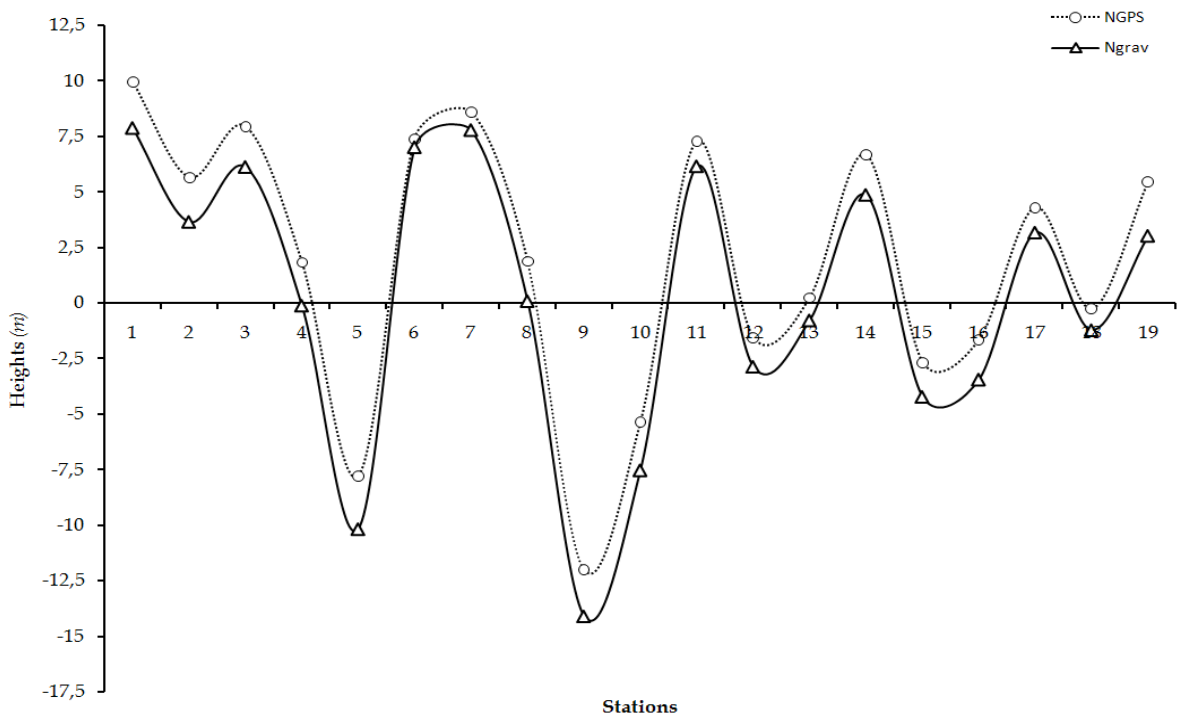

Figure 5.5: Gravimetric geoid heights with contribution of EIGEN-GRACE02S and the derived geoid heights by 19 GPS/levelling points.

In this study, to estimate the absolute accuracy of the KTH-SDG08 model we assume that the accuracies of the ellipsoidal and orthometric heights are ± 0.05 and $\pm 0.1\ m$, respectively. With uncorrelated errors we get:

$$\sigma^2_{N^{GPS/Lev}} = \sigma^2_h + \sigma^2_H \qquad (5.17)$$

and

$$\sigma^2_{\Delta N} = \sigma^2_N + \sigma^2_{N^{GPS/Lev}}, \qquad (5.18)$$

5.4.2. Verification of the geoid in relative sense

The standard deviation of the geoid height differences after the fitting was estimated at $\sigma_{\Delta N} = \pm 0.29m$. Hence, we have $\sigma_N = \pm 0.353\ m$ which can be taken as an estimate of the absolute accuracy of the gravimetric geoid model.

5.4.2 Verification of the geoid in relative sense

In case of geoid evaluation in relative sense, the orthometric and ellipsoidal height differences must be known. The main advantage of differencing is that any errors related to the baseline are cancelled, e.g. errors of vertical datum in long baselines; this could happen mainly over short distances of recent vertical datums than the older ones. Relative verification is basically used to assess the precision of the geoid gradient, which is given by subtracting the difference in orthometric height algebraically from the difference in ellipsoidal height. For this purpose, Equation (5.6) was used as follows:

$$\Delta H_{GPS-Geoid} = \Delta h_{GPS} - \Delta N_{Geoid} \tag{5.19}$$

where in ΔN_{Geoid} the gravimetric geoid values after the 7-parameter fitting is used, meaning that $\Delta N_{Geoid} = (N_2 - N_1) + (\varepsilon_2 - \varepsilon_1)$ (5.20)

Then the differences between two different orthometric height differences, i.e. from levelling (ΔH_{Ortho}) and from GPS minus Geoid $\left(\Delta H_{GPS-Geoid}\right)$, were derived:

$$\delta\Delta H_{Geoid-Level} = \Delta H_{GPS-Geoid} - \Delta H_{Level} \tag{5.21}$$

The relative differences between the GPS-geoid heights and the levelling heights becomes in part per million (ppm):

$$ppm = mean\left|\frac{\left(\delta\Delta H_{Geo-Level}\right)_{mm}}{D_{ij\,(km)}}\right| \tag{5.22}$$

where D_{ij} is the length of the baseline. The average distance between the 19 GPS/levelling points is $1120.944\ km$. Table 5.12 shows the results from the agreement between the relative values of the gravimetric and GPS/levelling derived geoid height. The new gravimetric model fits the GPS/levelling data with 0.493 *ppm.*

Table 5.12: The accuracy of the gravimetric geoid model in relative sense between the gravimetric geoid height and the derived geoid heights from GPS/levelling points.

No	ΔN *(m)*	Δh *(m)*	$\Delta H_{GPS/Lev-GEO}$ *(m)*	ΔH_{Level} *(m)*	δΔH *(m)*	D_{ij} *(m)*		ppm
1	-4.499	-102.957	-98.458	-98.648	0.190	276745.56	0.6849	0.6849
2	2.895	289.680	286.785	287.388	-0.603	296551.645	-2.0332	2.0332
3	-5.921	-481.765	-475.844	-475.653	-0.191	688347.614	-0.2775	0.2775
4	-9.431	-276.873	-267.442	-267.246	-0.196	997233.954	-0.1961	0.1961
5	15.795	-150.224	-166.019	-165.385	-0.634	1037936.05	-0.6106	0.6106
6	1.180	-9.076	-10.256	-9.703	-0.553	1079561.31	-0.5125	0.5125
7	-7.520	447.672	455.192	453.787	1.405	854363.142	1.6443	1.6443
8	-14.544	14.047	28.591	27.941	0.650	1404131.46	0.4630	0.4630
9	6.717	-402.913	-409.630	-409.562	-0.068	1147366.62	-0.0593	0.0593
10	13.780	26.522	12.742	13.868	-1.126	1243364.42	-0.9055	0.9055
11	-9.233	156.594	165.827	165.434	0.393	1171067.84	0.3353	0.3353
12	1.982	-68.989	-70.971	-70.781	-0.190	1177137.48	-0.1610	0.1610
13	6.485	2.778	-3.707	-3.653	-0.054	1331441.07	-0.0402	0.0402
14	-9.806	118.087	127.893	127.433	0.460	1302033.84	0.3534	0.3534
15	1.161	89.601	88.440	88.592	-0.152	1400334.05	-0.1087	0.1087
16	5.953	-261.649	-267.602	-267.612	0.010	1558401.57	0.0064	0.0064
17	-4.409	267.039	271.448	271.604	-0.156	1506381.14	-0.1039	0.1039
18	5.102	-361.310	-366.412	-367.043	0.631	1704598.18	0.3700	0.3700
Mean distance = 1120.944 km							**0.493** ppm	

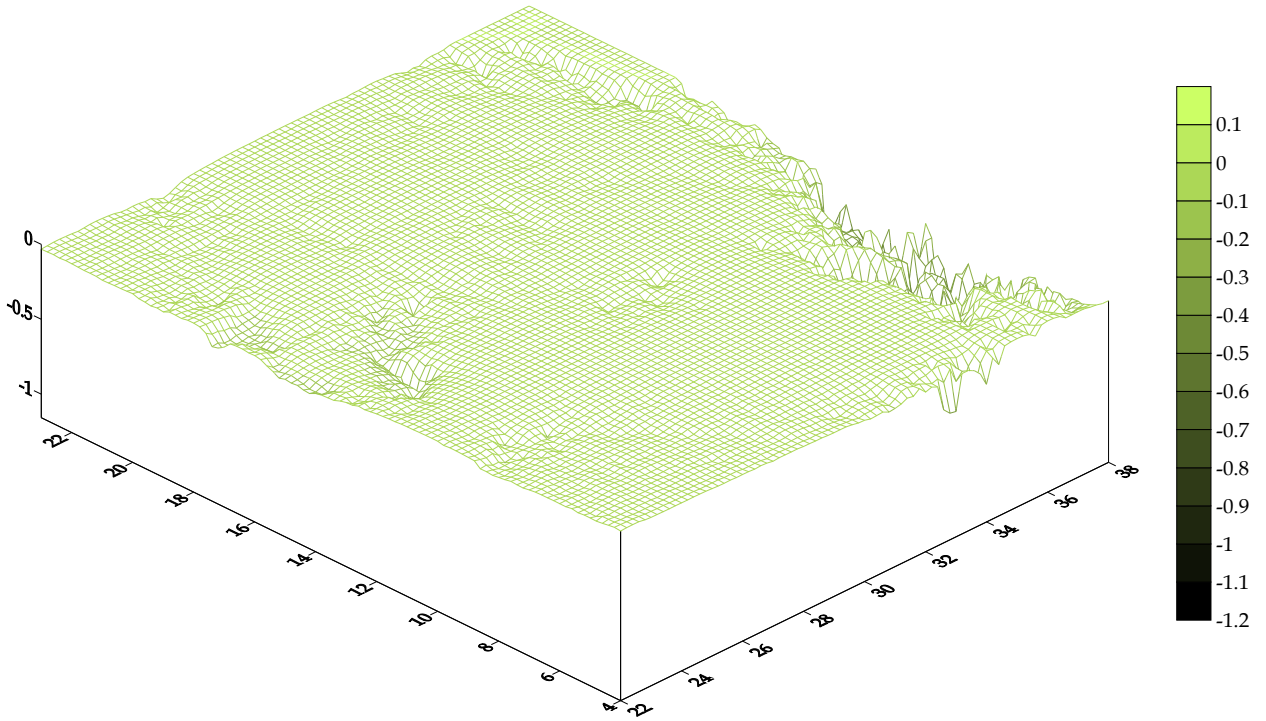

Figure 5.6: Combined topographic correction on the new Sudanese geoid model. Unit: m

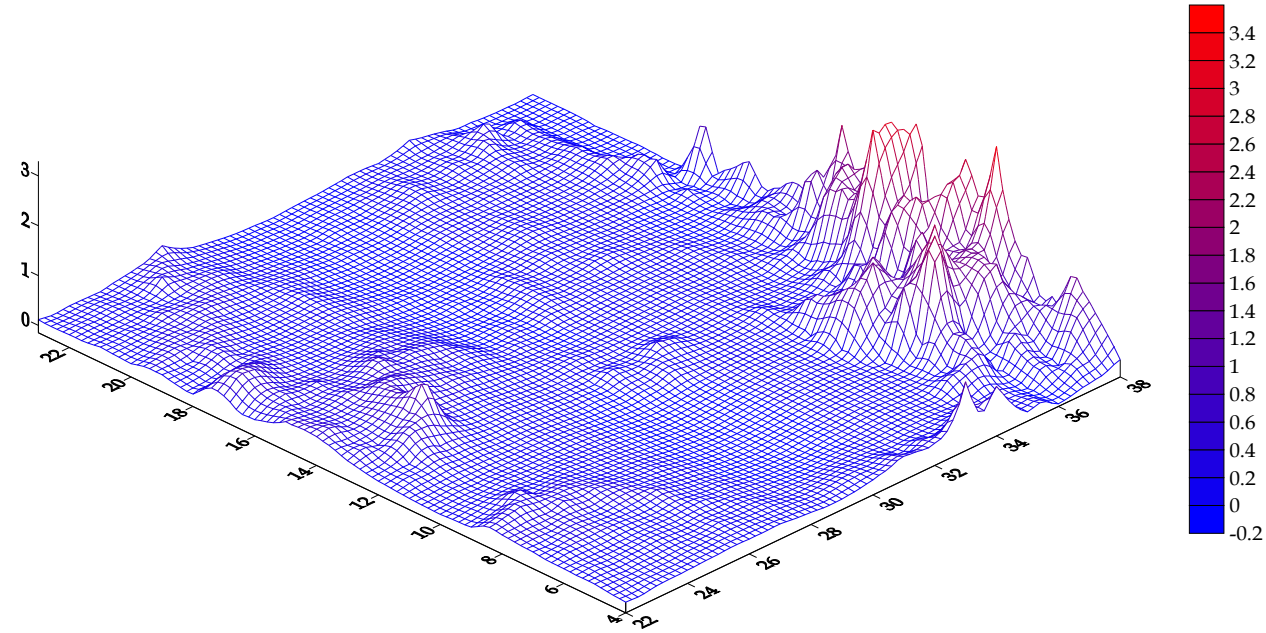

Figure 5.7: The downward continuation correction on the new geoid model. Unit: m

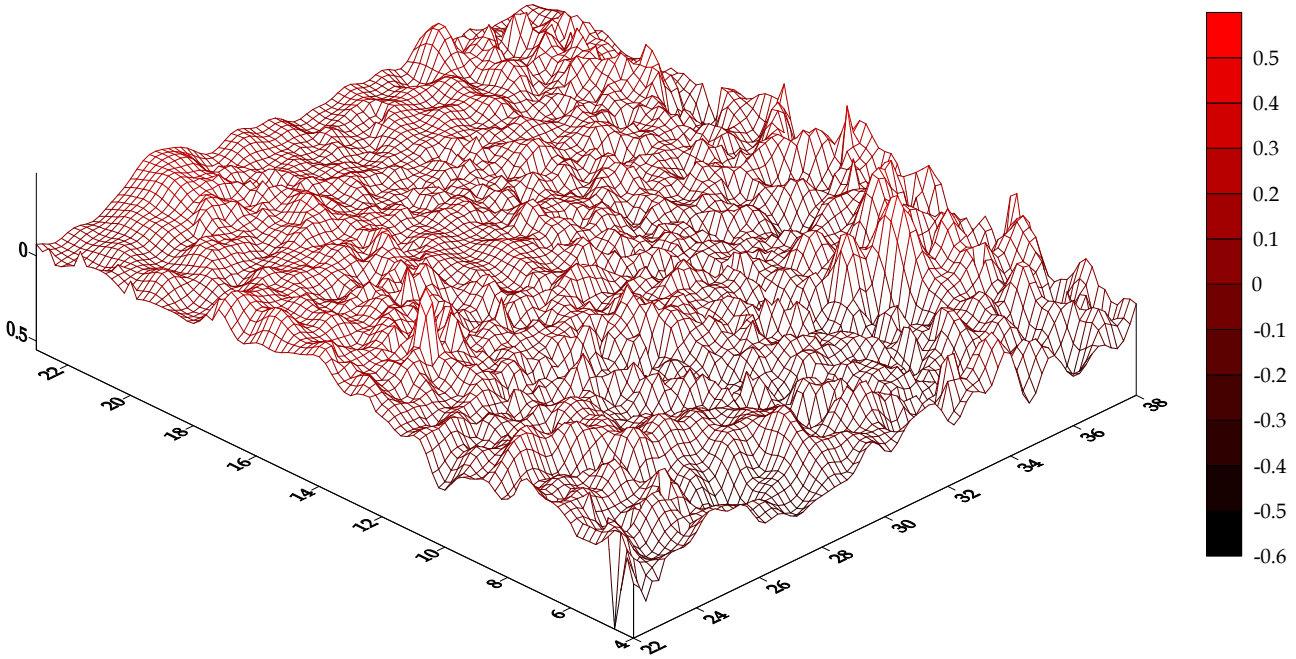

Figure 5.8: Ellipsoidal correction on the new Sudanese geoid model. Unit: mm

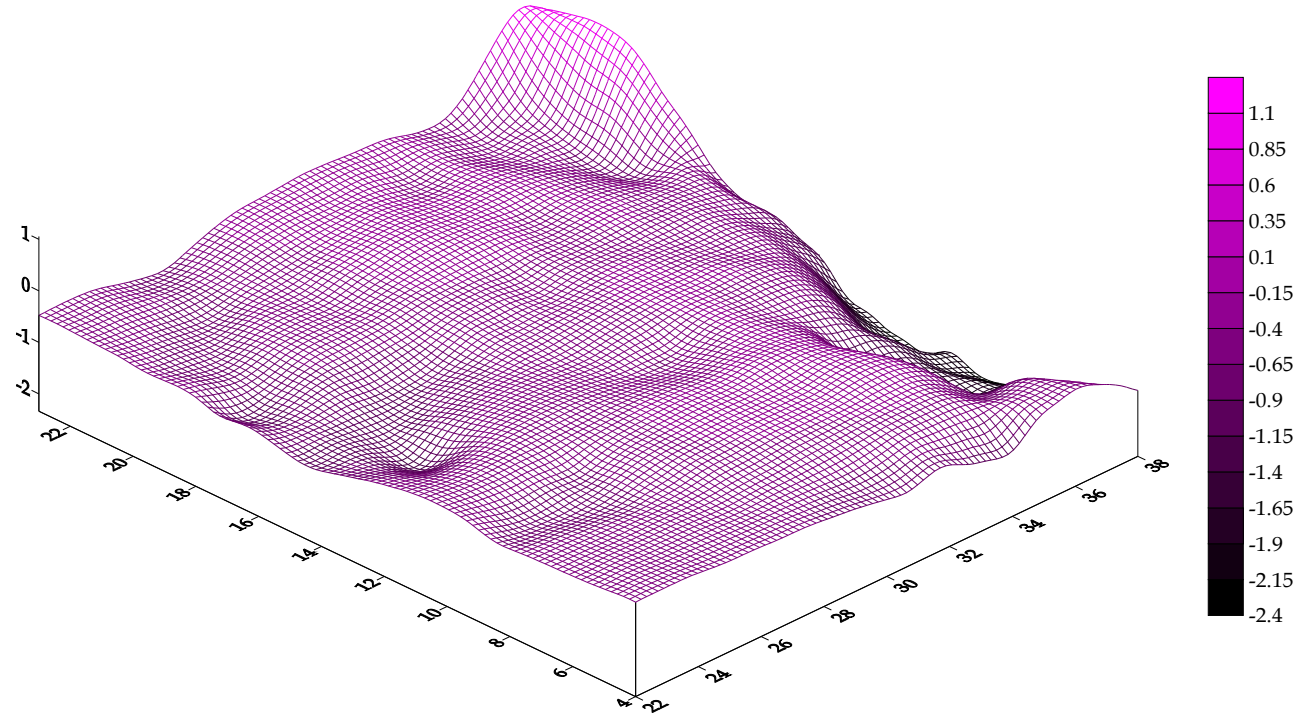

Figure 5.9: Combined atmospheric correction on the new Sudanese geoid model. Unit: mm

5.5 The new gravimetric geoid model (KTH-SDG08)

After deliberation and full investigations, by trying different interpolation methods for gridding Section 4.1.1, different GGMs Table 5.1, different values of terrestrial gravity anomaly accuracies Table 5.2 and different cap sizes Table 5.3. The new Geoid model of Sudan is computed based on free air gravity anomaly, GRACE02S gravitational model (satellite only) and 30″x 30″ SRTM DEM, located within the area $4^\circ \le \phi \le 23^\circ$, $22^\circ \le \lambda \le 38^\circ$.

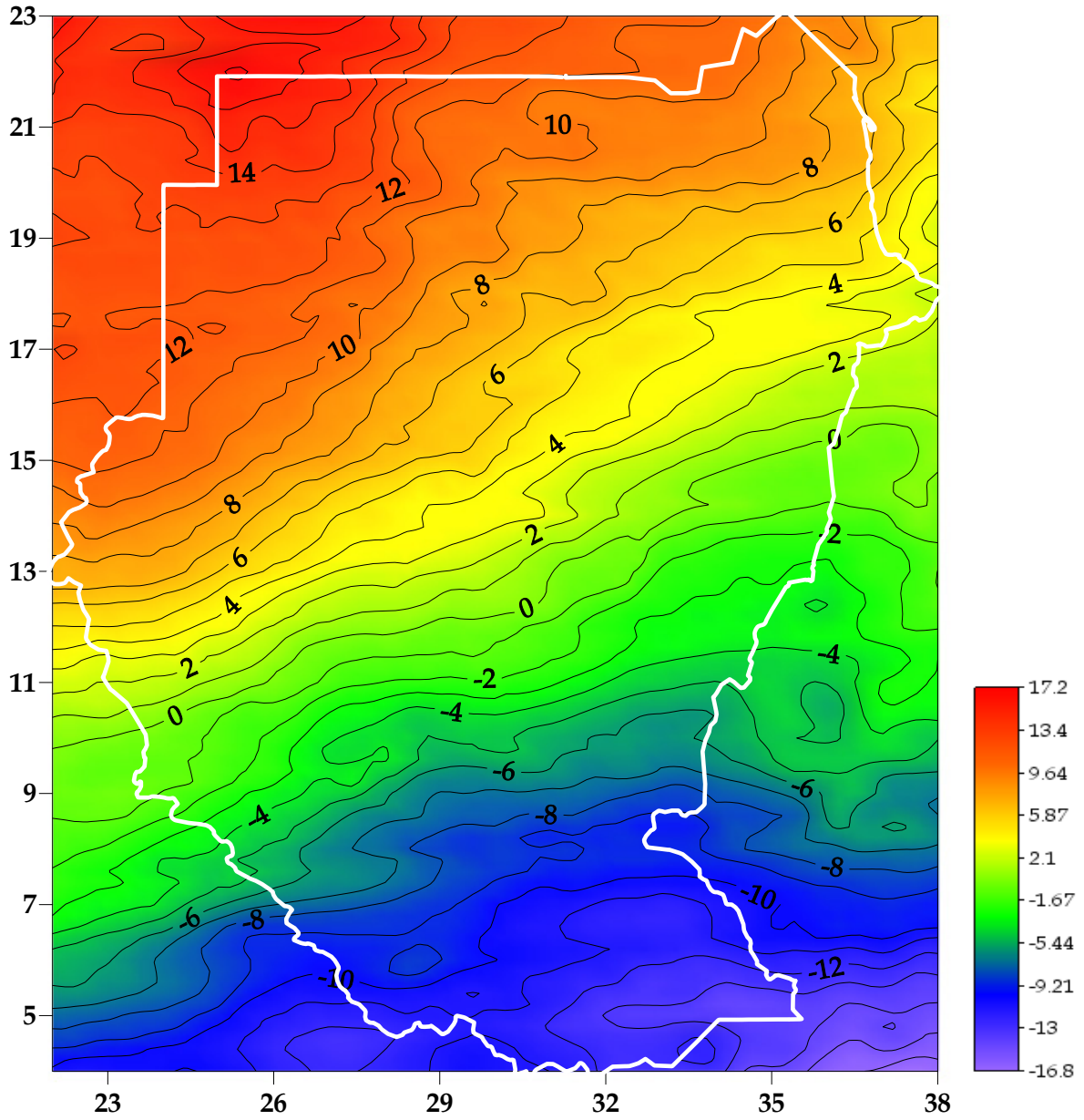

Figure 5.10: The new gravimetric geoid model (KTH-SDG08) of Sudan based on GRS80. Unit: m; Contour interval 1 m

The parameters that used to compute the final geoid model give the best result for the gravimetric geoid model against derived geoid height from GPS/levelling data. The additive corrections clarified in Chapter 3 were computed and added to the approximated geoid height. Figures 5.6-5.10 illustrate the additive corrections, the Combined Topographic, DWC, Ellipsoidal and Atmospheric Correction respectively. Figure 5.10 illustrates the contour map of the new geoid model. The correction for the variation of *GM* value in GRS80 reference ellipsoid and EIGEN-GRACE02S was taken to the account and added to Equation (3.1).

One may see from Figure 5.10, the geoid over Sudan is depreciating from the north-west to south-east as well as changing its sign from positive to negative in the same direction. The geoidal heights of (KTH-SDG08) reach drastic values in north-west corner and south-east corner are 17.2*m* and -16.8*m* respectively. The change of the sign of the (KTH-SDG08) heights spells out the fitting status with GRS80 reference ellipsoid. In northern part of the country, we find the ellipsoid is below the geoid, and then coincides with geoid diagonally from north-east to south-west border, and ultimately arises to be beyond the geoid in the small southern half of the country area.

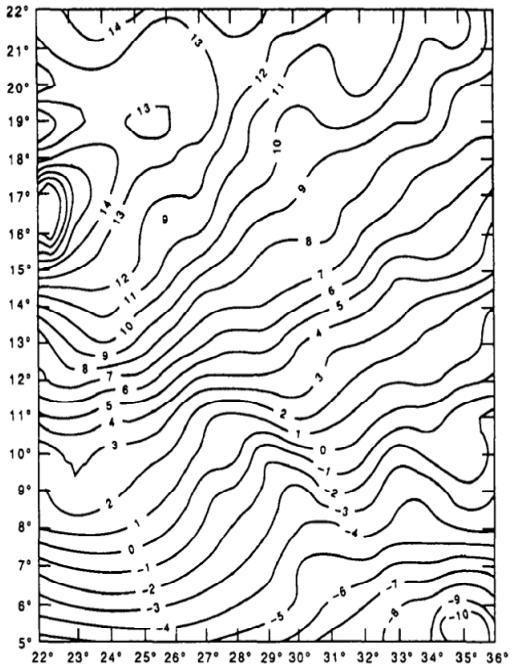

Figure 5.11.a The previous geoid model by Fashir 1991

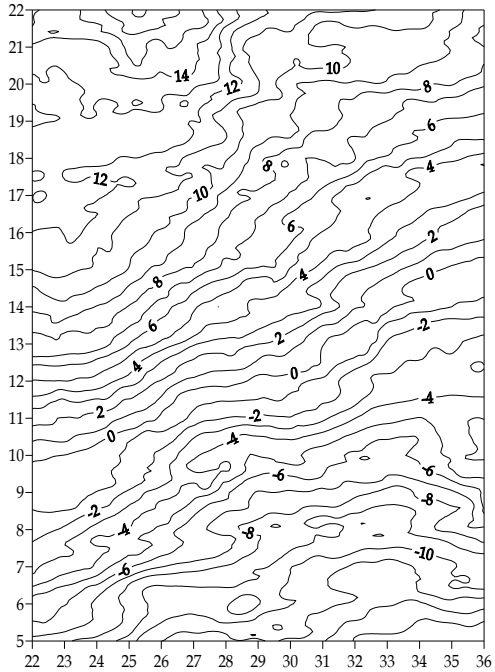

Figure 5.11.b The new geoid model (KTH-SDG08)

5.5. The New gravimetric Geoid Model (KTH-SDG08)

For sake of comparison, we tried to compare KTH-SDG08 with the previous model that computed by Fashir 1991. Unfortunately, we did not manage to obtain the evaluation data (Doppler data) that used by Fashir 1991. However, we decided to make a visual comparison by laying out both of them in the same size and providing general description. The KTH-SDG08 Figure 5.11.b was resized to $5^\circ \le \phi \le 22^\circ$, $22^\circ \le \lambda \le 36^\circ$ in order to be alike to Fashir's model size Figure 5.11.a. Generally the two models are not deviated so much. Fashir's model looks smoother than KTH-SDG08. The drastic values of the geoidal height in the north-west corner and south-east corner are *14 m* and -10 *m* for Fashir's model while 20 *m* and -14 *m* for KTH-SDG08, respectively. The fitting with the reference ellipsoid is similar from the north-west to south-east. Fashir's model covers the reference ellipsoid over a large area (approximately 75%). On the contrary KTH-SDG08 model apparently keeps the same fitting with reference ellipsoid as in the original area before resizing.

Chapter 6

Conclusions and Recommendations

In this study we attempted to determine the geoid model for Sudan by using the KTH method which combines different heterogeneous data in an optimum way. The new geoid model of Sudan has been computed by taking the following steps:

- The work started with collecting the fundamental data in the area of computation. The employed data in this study are; the gravity anomalies (GETECH and BGI), the SRTM DEM (30" x 30"), the GGM and 19 GPS/levelling points were provided.

- The gravity data has been evaluated and refined through two tests, in order to choose the optimal available data. The first test based on cross validation approach was applied to detect the outliers points and consequently 213 points were ignored from the dataset, based on the value of the tolerance point of the interpolation error which set to avoid all points error > *60 mGal*. In addition 20 points have been deleted in the second test that performed to compare the gravity anomalies of Molodensky with the gravity anomalies computed by EIGEN-GL04C gravitational model. Three Different interpolation algorithms (*kriging*, *inverse distance weighting* and *nearest neighbor*) were tested for final gridding, *kriging* was best one for constructing the final 5'x 5' gravity anomaly grid with 3° offset out the computation area (outer zone).

- Among 4 GGMs inquired into comparison with the GPS/levelling data to find which one has the best agreement. EIGEN-GRACE02S (satellite only) is the best model to fit the GPS/levelling data with accuracy of 0.29. EIGEN-GL04C (combined model) has also closest result 0.32 *m*. However, from a theoretical point of view the EIGEN-GRACE02S is used in LSM method due to the fact that the higher degree GGMs composed terrestrial gravity data as well as the power of GGMs is in low degrees. Hence the terrestrial data may be used twice in case of using combined model; therefore we preferred using EIGEN-GRACE02S (satellite only) to avoid this correlation, overall both models are identical according to the achieved numerical results.

6.1. Recommendations for future work

- After constructing the gravity anomaly grid data, an approximate geoid height was computed by using stochastic least-squares modification methods of Stokes' formula proposed by Sjöberg. Both gravity anomaly data and the GGM were combined in the modified formula beside the least-squares modification parameters. After that the additive corrections of the KTH method were computed and added to the approximate geoid height, yielding the corrected geoid height.

- Finally, the assessment of the new gravimetric geoid has been done in absolute sense by computing the global mean square error as an internal accuracy, while the external accuracy determined by comparing with GPS/levelling in term of relative sense. The standard deviation is served as an indication of accuracy in absolute sense, in this study the standard deviation of the agreement between the new geoid and *19* GPS/levelling points after 7-parameter fitting is estimated to $0.29\,m$. The additive corrections have improved the standard deviation of the final gravimetric geoid height after using 7-Parameter fitting to become $0.29\,m$ instead of $0.42\,m$ of the uncorrected geoid heights. Because of the fact that GPS/levelling data comprises some systematic errors and inconsistencies between vertical datums, the actual potential of the geoid could not always be indicated by absolute view. On the contrary the GPS/levelling data is very efficient and has perfect accuracy in relative sense, much more systematic errors are decimated by differencing, hence the relative accuracy based on $\Delta H_{GPS-Geo}$ against the levelling data shows that the fitting between the new geoid and GPS/levelling is $0.493\,ppm$.

By comparing with relevant existed model which computed in 1990 and on basis of available information (only values of standard deviations), it has been found that the current geoid model for Sudan appears with an improved external accuracy by having ± 0.29 m instead of ± 1.88 m for the model computed in 1991 and evaluated by 83 Doppler points.

6.1 Recommendations for future work

The main restrictions in this study is the data acquisition, after hardship the collected gravity data only represents *33%* of the total required data for the outer zone (3° offset). The destitution of the gravity data coverage in Sudan can be apparently seen through the un-surveyed areas as well as gabs between surveyed areas, Figure 4.1, the total area of Sudan is 2,505,810 km^2, by referring to the total of the gravity data we find that one gravity point per 106 km^2, therefore un-surveyed areas (area without terrestrial gravity data) were filled by gravity anomalies derived by EIGEN-GL04C. Moreover, additional gravity data is required from neighboring countries and ship-borne data of the Red Sea to obtain more accurate geoid height towards 1 cm geoid accuracy. Due to large area of Sudan it is difficult to cover the whole country area with terrestrial gravity data. In this case air-borne surveys would overcome problems of laborious and high cost as well as for the mountainous areas. Particularly, transportations in Sudan do not connect and reach all remote areas.

A result of Aerial photography campaign for Merowe Dam construction (located to the north part of the country) in 2000 reveals discrepancies of ± 0.6 m in control points of first and second order over there, therefore a new unified reference system with dense control points should be carried out to cope with the new revolution of accuracy, it is also recommended to be referred to a compatible reference ellipsoid, other control points in old geodetic network are suspected to have some deficiencies unless evaluation encountered.

Furthermore, GPS ellipsoidal heights should be co-located with control points of triangulation networks particularly in remote zones and mountainous areas and all around the country area. Perfect diffusion of the GPS/levelling data in region of geoid is considerable in providing a meaningful verification to the gravimetric geoid model.

DEM contribution is important in KTH methods by virtue of its utilization in topographic and downward continuation corrections those demanded, errors in DEM bring out immediate errors to the gravity anomalies at interpolation of bouguer gravity anomalies, and errors also affected the geoid models by DEM's contribution in DWC and topographic correction. Consequently, evaluation of DEM has a matter of importance before it used in the geoid determination.

Bibliography

Adam MO (1967): *A Geodetic Datum for the Sudan*. (Master's Thesis), Cornell University, USA.

Amos MJ and Featherstone WE. (2003): *Preparation for a new gravimetric geoid model of New Zealand, and some preliminary results*. New Zealand Surveyor, No.293.

C.C.Tscherning, Anwar Radwan, A.A.Tealeb, S.M.Mahmoud, Abd El-monum Mohamed, Ramdan Hassan, El-Syaed Issawy and K. Saker. (2001): *Local geoid determination combining gravity disturbances and GPS/levelling A case study in the Lake Naser area, Aswan, Egypt*. Journal of Geodesy, 75:343-348.

Denker, H., J.-P. Barriot, R. Barzaghi, R. Forsberg, J. Ihde, A. Kenyeres, U. Marti, I.N. Tziavos (2004): *Status of the European Gravity and Geoid Project EGGP*. Newton's Bulletin, No. 2, 87-92.

Ellmann A (Submitted): *Effect of GRACE Satellite mission to gravity field studies in Fennoscandia and the Baltic Sea region*. Proc. Estonia Acad. Sci. Geol.

Ellmann A. (2001): *Least squares modification of Stokes' formula with applications to the Estonian geoid*. Royal Institute of Technology, Division of Geodesy Report No. 1056 *(Licentiate Thesis),* Stockholm.

Ellmann A. (2002c): *An improved gravity anomaly grid and a geoid model for Estonia* Proc. *Estonia Acad. Sci. Geol*., 51: 199-214.

Ellmann A. and Sjöberg LE (2002e): *Combined topographic effect applied to biased type of modified Stokes formula*. Boll. Geod. Sci. Aff., 61: 207-226.

Ellmann A. and Sjöberg LE (2004): *Ellipsoidal correction for the modified Stokes formula*. Boll. Geod. Sci. Aff., 63(No.3).

Ellmann A. (2005a): *Computation of three stochastic modifications of Stokes's formula for regional geoid determination*. Computers and Geosciences, 31/6, pp.742-755.

Ellmann A. (2005b): *Two deterministic and three stochastic modifications of Stokes's formula: a case study for the Baltic countries*. Journal of Geodesy, 79, 11-23.

Fan H. (1998): *On an Earth ellipsoid best-fitted to the Earth surface*. Journal of Geodesy, 72(3):154-160.

Bibliography

Fan H (2002): *Development of the Mozambican geoid model MOZGEO 2002,* Geodesy research No. 1058, The Royal Institute of Technology, Stockholm, Sweden.

Fan H (2006): *Theoretical Geodesy*. Geodesy report No.2016, The Royal Institute of Technology, Stockholm, Sweden.

Fashir HH. (1991): *The Gravimetric Geoid of Sudan*. Journal of Geodynamics, Vol.14, NOS 1-4, PP.19-36, 1991.

Featherstone WE (2001): *Absolute and relative testing of gravimetric geoid models using Global Positioning System and orthometric height data*. Computer & Geosciences, Vol.27, 807-814.

Featherstone WE and Sproule DM (2006): *Fitting AUSGeoid98 to the Australian Height Datum using GPS data and least squares collocation: application of a cross-validation technique*, Survey Review 38(301):573-582.

Ghanem E. (2001): *GPS-Gravimetric Geoid Determination in Egypt*. Geospatial Information Science, Vol.4, No.1, P. 19-23.

Geisser S., and Eddy W.F., (1979): *A predictive approach to model selection. Journal of the American Statistical Association,* 74(365), 153-160.

GETECH (2008): *Gravity point data for Sudan, Geophysical Exploration Technology (GETECH)*, University of Leeds.

Heck B. (1990): *An evaluation of some systematic error sources affecting terrestrial gravity anomalies*. Bulletin Géodésique, 64, 88-108.

Heiskanen WA, Moritz H (1967): *Physical Geodesy*. W H Freeman and Co., New York, London and San Francisco.

Hofmann-Wellenhof B and Moritz H (2006), *Physical Geodesy*, Second edition, Springer-Verlag Wien.

Hunegnaw Addisu (1997): *Local geoid determination by gravimetric methods and GPS/levelling: A case study in the Ethiopian Rift Valley*. (Master's thesis). The Royal Institute of Technology, Stockholm, Sweden.

Ibrahim A (1993): *Interpretation of Gravity and magnetic data from the Central African Rift system [Sudan]*: (Ph.D. Thesis), University of Leeds.

Kiamehr R (2005a): *Qualification and refinement of the gravity database based on cross-validation approach, A case study of Iran*, Proc Geomatics 2004 (84) Conferences, National Cartographic Centre of Iran, Teheran, Iran, Revised version, submitted J. Acta Geodaetica et Geophysica.

Bibliography

Kiamehr R and Sjöberg LE (2005b): *Effect of the STRM global DEM on the determination of a high-resolution geoid model: A case study in Iran*, Journal of Geodesy, 79(9):540-551.

Kiamehr R (2006a): *A strategy for determining the regional geoid in developing countries by combining limited ground data with satellite-based global geopotential and topographical models: A case study of Iran*, Journal of Geodesy, 79(10,11):602-612.

Kiamehr R (2006b): *Hybrid precise gravimetric geoid model for Iran based on recent GRACE and STRM data and the least squares modification of Stokes' formula*, J. Physics of Earth and Space, 32(1):7-23.

Kiamehr R (2006c): *The impact of lateral density variation model in the determination of precise gravimetric geoid in mountainous areas: A case study of Iran*, in press Geophysical Journal International.

Kiamehr R (2006d): *Precise Gravimetric Geoid Model for Iran Based on GRACE and SRTM Data and the Least-Squares Modification of Stokes' Formula: with Some Geodynamic Interpretations*, (Ph.D. Thesis), The Royal Institute of Technology, Stockholm, Sweden.

Kotsakis C, Sideris MG (1999): *On the adjustment of combined GPS/levelling/geoid networks*. Journal of Geodesy, Vol 73(8), 412-421.

Nsombo Peter (1996): *Geoid determination over Zambia*. (Ph.D Thesis), The Royal Institute of Technology, Stockholm, Sweden.

Rapp RH and Pavlis NK (1990): *The development and analysis of geopotential coefficients models to spherical harmonic degree 360*, J. Geophys. Res, 95(B13)21885-21911.

Reigber Christoph, Schmidt Roland, Flechtner Frank, König Rolf, Meyer Ulrich, Neumayer Karl-Hans, Schwintzer Peter, Sheng Yuan Zhu (2005): *An Earth gravity field model complete to degree and order 150 from GRACE: EIGEN-GRACE02S*, Journal of Geodynamics 39(1), 1-10.

R.S. Grebenitcharsky, E.V. Rangelova and M.G. Sideris (2005): *Transformation between gravimetric and GPS/levelling-derived geoids using additional gravity information*. Journal of Geodynamics, Vol.39, 527-544.

S.A. Benahmed Daho, J.D. Fairhead, A. Zeggai, B. Ghezali, A. Derkaoui, B. Gourine and S. Khelifa, *A new investigation on the choice of the tailored geopotential model in Algeria*, Journal of Geodynamics 45 (2–3) (2008), pp. 154–162.

Sjöberg LE (1998): *The atmospheric geoid and gravity corrections*. Boll Geod Sci Aff, 57(4):421-435.

Sjöberg LE (1999a)*: On the downward continuation error at the Earth's surface and the geoid of satellite derived geopotential models*. Boll Geod Sci Affini 58(3):215-229.

Bibliography

Sjöberg LE (1999b): *The IAG approach to the atmospheric geoid correction in Stokes formula and a new strategy*. Journal of Geodesy, 73(7):362-366.

Sjöberg LE and Hunegnaw A (2000): *Some modifications of Stokes' dormula that account for truncation and potential coefficients errors*. Journal of Geodesy, 74:232-238.

Sjöberg LE (2001a): *Topographic and atmospheric corrections of gravimetric geoid determination with special emphasis on the effects of degree zero and one*. Journal of Geodesy, 75:283-290.

Sjöberg LE (2001b): *The effect of downward continuation of gravity anomaly to the sea-level in Stokes' formula*. Journal of Geodesy, 74:796-804.

Sjöberg LE (2003a): *A solution to the downward continuation effect on the geoid determined by Stokes' formula*. Journal of Geodesy, 77:94-100.

Sjöberg LE (2003b): *Improving modified Stokes' formula by GOCE data*. Boll Geod Sci Aff 61(3):215-225.

Sjöberg LE (2003c): *A computational scheme to model geoid by the modified Stokes formula without gravity reductions*. Journal of Geodesy, 74:255-268.

Sjöberg LE (2003d): *A general model of modifying Stokes' formula and its least squares solution*. Journal of Geodesy, 77:459-464.

Sjöberg LE (2003e): *The ellipsoidal corrections to the topographic geoid effects*. Journal of Geodesy, 77:804-808.

Sjöberg LE (2004): *A spherical harmonic representation of the ellipsoidal correction to the modified Stokes formula*, Journal of Geodesy, 78(3):1432-1394.

Sjöberg LE (2006): *The effects of Stokes' formula for an ellipsoidal layering of the Earth's atmosphere*. Journal of Geodesy, 79(12):675-681.

Sjöberg LE and Featherstone WE (2004): *Two-step procedures for hybrid geoid modelling*. Journal of Geodesy, Vol.78, 66-75.

Tscherning, C., Rapp, R., (1974): *Closed covariance expressions for gravity anomalies, geoid undulations and deflections of the vertical implied by anomaly degree variance models*. Report No. 208, Department of Geodetic Science, Ohio State University, Columbus, OH.

V. Corchete, M. Chourak and D. Khattach, *The high-resolution gravimetric geoid of Iberia: IGG2005*, Geophys. J. Int. 162 (2005), pp. 676–684.

V. Corchete and M.C. Pacino (2007): *The first high-resolution gravimetric geoid for Argentina: GAR*. Physics of the Earth and Planetary Interiors, Vol.161, 177-183.

Bibliography

Ågren J (2004): *Regional geoid determination methods for the era of satellite gravimetry*, (Ph.D. Thesis), Royal Institute of Technology, Stockholm, Sweden.

Reports in Geographic Information Technology 2006-2009

The TRITA-GIT Series - ISSN 1653-5227

2006

06-001 **Uliana Danila**. Corrective *surface for GPS-levelling in Moldova*. Master of Science thesis in geodesy No. 3089. Supervisor: Lars Sjöberg. TRITA-GIT EX 06-001. January 2006.

06-002 **Ingemar Lewén**. *Use of gyrotheodolite in underground control network*. Master of Science thesis in geodesy No. 3090. Supervisor: Erick Asenjo. TRITA-GIT EX 06-002. January 2006.

06-003 **Johan Tornberg**. *Felfortplantningsanalys i GIS-projekt genom Monte Carlo-simulering*. Master of Science thesis in geoinformatics. Supervisor: Mats Dunkars. TRITA-GIT EX 06-003. February 2006.

06-004 **Constantin-Octavian Andrei**. *3D affine coordinate transformations*. Master of Science thesis in geodesy No. 3091. Supervisor: Huaan Fan. TRITA-GIT EX 06-004. March 2006.

06-005 **Helena von Malmborg**. *Jämförelse av Epos och nätverks-DGPS*. Master of Science thesis in geodesy No. 3092. Supervisor: Milan Horemuz. TRITA-GIT EX 06-005. March 2006.

06-006 **Lina Ståhl**. *Uppskattning av kloridhalt i brunnar - modellering och visualisering med hjälp av SAS-Bridge*. Master of Science thesis in geoinformatics. Supervisor: Hans Hauska. TRITA-GIT EX 06-006. May 2006.

06-007 **Dimitrios Chrysafinos**. *VRS network design considerations applicable to the topology of the Hellenic Positioning System (HEPOS) stations*. Master of Science thesis in geodesy No.3093. Supervisor: Lars Sjöberg. TRITA-GIT EX 06-007. May 2006.

06-008 **Tao Zhang**. *Application of GIS and CARE-W systems on water distribution networks*. Master of Science thesis in geoinformatics. Supervisor: Mats Dunkars. TRITA-GIT EX 06-008. May 2006.

06-009 **Krishnasamy Satish Kumar**. *Usability engineering for Utö tourism information system*. Master of Science thesis in geoinformatics. Supervisor: Mats Dunkars. TRITA-GIT EX 06-009. May 2006.

06-010 **Irene Rangle**. *High resolution satellite data for mapping Landuse/land-cover in the rural-urban fringe of the Greater Toronto area*. Supervisor: Yifang Ban. TRITA-GIT EX 06-010. May 2006.

06-011 **Kazi Ishtiak Ahmed**. ENVISAT *ASAR for land-cover mapping and change detection*. Supervisor: Yifang Ban. TRITA-GIT EX 06-011. May 2006.

06-012 **Jian Liang**. *Synergy of ENVISAT ASAR and MERIS data for landuse/land-cover classification*. Supervisor: Yifang Ban. TRITA-GIT EX 06-012. May 2006.

06-013 **Assad Shah**. *Systematiska effecter inom Riksavvägningen*. Master of Science thesis in geodesy No.3094. Supervisor: Tomas Egeltoft. TRITA-GIT EX 06-013. August 2006.

06-014 **Erik Trehn**. *GPS Precise Point Positioning – An Investigation In Reachable Accuracy*. Master of Science thesis in geodesy No.3095. Supervisor: Milan Horemuz. TRITA-GIT EX 06-014. August 2006.

2007

07-001 **Carl Schedlich**. *Turn at the roundabout: A practical assessment of spatial representations in two different GPS interfaces from a pedestrian's perspective*. Bachelor of Science thesis in geoinformatics. Supervisor: Michael Le Duc. January 2007.

07-002 **Staffan Bengtsson**. *Förändringsanalys i ortofoton*. Master of Science thesis in geoinformatics. Supervisor: Jonas Nelson and Patric Jansson. TRITA-GIT EX 07-002. March 2007.

07-003 **Joseph Addai**. *Qantification of temporal changes in metal loads – Moss data over 20 years*. Master of Science thesis in geoinformatics. Supervisor: Katrin Grunfeld. March 2007.

07-004 **Stephen Rosewarne**. *Deformation study of the Vasa Ship*. Bachelor of Science thesis in geodesy No.3097. Suppervisor: Milan Horemuz. March 2007.

07-005 **Naeim Dastgir**. *Processing SAR Data Using Range Doppler and Chirp Scaling Algorithms*. Master of Science thesis in geodesy No.3096. Supervisor: Lars Sjöberg. April 2007.

07-006 **Torgny Israelsson** and **Youssef Shoumar**. *Motion Detection with GPS*. Master of Science thesis in geodesy No.3098. Supervisor: Milan Horemuz. April 2007.

07-007 **Akjol Djenaliev**. *Multicriteria decision making and GIS for railroad planning in Kyrgyzstan*. Master of Science thesis in geoinformatics. Supervisor: Hans Hauska. May 2007.

07-008 **Anna Hammar**. *Quality comparison of automatic 3D city house modelling methods from laser data*. Master of Science thesis in geodesy No.3099. Supervisor: Milan Horemuz. May 2007.

07-009 **Md Ubydul Haque**. *Mapping malaria vector habitats in the dry season in Bangladesh using Spot imagery*. Master of Science thesis in geoinformatics. Supervisor: Hans Hauska. May 2007.

07-010 **Jing Jiang**. *Analysis of the Suitable and Low-Cost Sites for Industrial Land Using Multi Criteria Evaluation: A Case of Panzhihua, China*. Master of Science thesis in geoinformatics. Supervisor: Yifang Ban. June 2007.

07-011 **Raghavendra Jayamangal**. *Quantification of coastal erosion along Spey Bay and the Spey River using photogrammetry and LiDAR imagery-derived DTMs*. Master of Science thesis in geoinformatics. Supervisor: Yifang Ban and Jim Hansom. June 2007.

07-012 **Alicia E. Porcar Lahoz**. *An analysis of how geographical factors affect real estate prices*. Master of Science thesis in geoinformatics. Supervisor: Yifang Ban. October 2007.

07-013 **Ebenezer Kwakye Bentum**. *Detection of land use change in the Accra Metropolitan Area from 1990 to 2000*. Master of Science thesis in geoinformatics. Supervisor: Hans Hauska. November 2007.

07-014 **Jesper Gradin**. *Aided inertial navigation field tests using an RLG IMU*. Master of Science thesis in geodesy No.3100. Supervisor: Milan Horemuz. December 2007.

2008

08-001 **Wan Wen**. Road Roughness Detection by analyzing IMU Data. Master of Science thesis in geodesy No.3101. Supervisor: Milan Horemuz. Janaury 2008.

08-002 **Ilias Daras**. Determination of a gravimetric geoid model of Greece using the method of KTH. Master of Science thesis in geodesy No.3102. Supervisor: Huaan Fan and Kalliopi Papazissi. Janaury 2008.

08-003 **Anwar Negash Surur**. Surveying, modelling and visualisation of geological structures in the Tunberget tunnel. Master of Science thesis in geoinformatics. Supervisor: Hans Hauska. February 2008.

08-004 **Helena Swanh**. Noggrannhetskontroll av data 3D-modell från pulsskanner och fasmätningsskanner. Master of Science thesis in geodesy No.3103. Supervisor: Milan Horemuz. March 2008.

08-005 **Henrik Löfqvist**. Inpassning av mätdata i inhomogena nät. Master of Science thesis in geodesy No.3104. Supervisor: Milan Horemuz and Anders Viden. April 2008.

08-006 **Cement Takyi**. Lineament study in the Björkö area using satellite radar and airborne VLF data - possible tools for groundwater prospecting. Master of Science thesis in geoinformatics. Supervisor: Herbert Henkel. June 2008.

08-007 **Qarin Bånkestad.** 3D data: Faktisk hantering för att kunna lagra, återfå och visualisera tredimensionell information. Master of Science thesis in geoinformatics. Supervisor: Hans Hauska. June 2008.

08-008 **Tadesse Tafesse Kebede**. Development and implementation of filter algorithms and controllers to a construction machine simulator. Master of Science thesis in geodesy No.3105. Supervisor: Lars Sjöberg. September 2008.

08-009 **Gulilat Tegane Alemu**. Assessments of effects on mixing different types of GPS antennas and receivers. Master of Science thesis in geodesy No.3106. Supervisor: Lars Sjöberg. September 2008.

08-010 **Jure Kop**. Tests of New Solutions to the Direct and Indirect Geodetic Problems on the Ellipsoid. Master of Science thesis in geodesy No.3107. Supervisor: Lars Sjöberg. September 2008.

08-011 **Karoliina Kolehmainen**. Monitoring and Analysis of Urban Land Cover Changes over Stockholm Region between 1986 and 2004 using Remote Sensing and Spatial Metrics. Master of Science thesis in geoinformatics. Supervisor: Yifang Ban. October 2008.

08-012 **Johan Wallin**. Land-Cover Mapping in Stockholm Using Fusion of ALOS PALSAR and SPOT Data. Master of Science thesis in geoinformatics. Supervisor: Yifang Ban. October 2008.

08-013 Mårten Korall. A comparison between GNSS, Laser scanning and Photogrammetry for volume calculation of aggregates and gravel materials. Master of Science thesis in geodesy No.3108. Supervisor: Milan Horemuz. December 2008.

2009

09-001 **Ahmed Abdallah.** Determination of a gravimetric geoid if Sudan using the KTH method. Master ofScience thesis in geodesy No.3109. Supervisor: Huaan Fan. Janaury 2009.